International Journal of Bifurcation and Chaos, Vol. 16, No. 3 (2006) 647–669

BASIN FRACTALIZATIONS GENERATED BY A TWO-DIMENSIONAL FAMILY OF (Z_1–Z_3–Z_1) MAPS

GIAN-ITALO BISCHI* and LAURA GARDINI†
Istituto di Scienze Economiche,
University of Urbino, Italy
**bischi@econ.uniurb.it*
†*gardini@econ.uniurb.it*

CHRISTIAN MIRA
CESNLA 19 rue d'Occitanie, Fonsegrives, 31130 QUINT,
and Istituto di Scienze Economiche,
University of Urbino, Italy
c.mira@free.fr

Received January 11, 2005; Revised February 14, 2005

Two-dimensional (Z_1–Z_3–Z_1) maps are such that the plane is divided into three unbounded open regions: a region Z_3, whose points generate three real rank-one preimages, bordered by two regions Z_1, whose points generate only one real rank-one preimage. This paper is essentially devoted to the study of the structures, and the global bifurcations, of the basins of attraction generated by such maps. In particular, the cases of fractal structure of such basins are considered. For the class of maps considered in this paper, a large variety of dynamic situations is shown, and the bifurcations leading to their occurrence are explained.

Keywords: Dynamical systems; noninvertible maps; critical curves; basins of attraction; global bifurcations.

1. Introduction

This paper is devoted to some properties of a family of (Z_1–Z_3–Z_1) two-dimensional noninvertible maps $T : (x, y) \to (x', y')$, defined by two polynomials, a linear one and a cubic one, in the form:

$$\begin{aligned} x' &= x + y \\ y' &= ax + bx^2 + cx^3 + dy \end{aligned} \tag{1}$$

This family of maps depends on the parameters a, b, c, d. It is reminded that noninvertible maps are identified by a symbolism based on the configuration of regions Z_k of the space, each point of Z_k having k distinct rank-one real preimages (see e.g. [Mira *et al.*, 1996a]). For the two-dimensional map (1), (Z_1–Z_3–Z_1) means that the plane is divided into three unbounded open regions: a region Z_3, whose points generate three real rank-one preimages, bordered by two regions Z_1, whose points generate only one real rank-one preimage. The map family considered here is such that the boundaries of the regions Z_k, $k = 1, 3$, are made up of two parallel straight lines L, L'. These lines are the branches of the rank-one critical curve $LC = L \cup L'$, locus of points such that two determinations of the inverse correspondence T^{-1} are merging on the set $LC_{-1} = L_{-1} \cup L'_{-1}$, which is made up of two vertical parallel straight lines. The set LC_{-1} is the locus of points where the Jacobian determinant of T vanishes. For the maps (1) the plane may be considered as made up of k sheets inside Z_k, $k = 1, 3$, the sheets joining along the set LC. This is related to what is called a *foliation* of the plane [Mira *et al.*, 1996a;

Mira *et al.*, 1996b; Cathala, 2003]. *It is worth noting that noninvertible polynomial maps are incompletely identified by their degree.* Indeed, two-dimensional quadratic maps may lead to regions Z_k, for which the highest integer k is either 2 or 4. For two-dimensional maps with cubic components the highest integer k may be either 3, or 5, or 7, or 9. The map complexity depends on the highest value of k. So a good map identification implies the recognition of the Z_k regions ($k = 1, 3$, here) configuration. The (Z_1–Z_3–Z_1) foliation structure is the simplest one for cubic maps. More complex situations occur when LC contains cusp points, represented by a symbol "<", or ">". So if the highest value of k is three, ($Z_1 < Z_3$) maps are such that LC (separating only two areas Z_1 and Z_3) has a cusp ("cape") "penetrating" in Z_1. Maps of ($Z_1 < Z_3 >$) type are defined by LC as a closed curve containing Z_3, with two cusp points, giving rise to a "lip" shape. Such arguments, with several examples, are developed in [Mira *et al.*, 1996a]. When the inverse map has a vanishing denominator along a curve (γ), the boundary of regions Z_k are made up of branches of LC, but also may be constituted by arcs of (γ) (see [Bischi *et al.*, 1999, p. 147]).

This paper is essentially devoted to the basin structures generated by T, more particularly when they are fractal, and their bifurcations. For the maps considered here, a large variety of dynamic situations is shown, and the bifurcations leading to their occurrence are explained. Taking into account the complexity of the corresponding problems, the modus operandi is not an abstract one. It imitates the botanists approach, collecting piece by piece unknown plants, hoping to find relations between some of them in order to define classes of properties. In the present case the identification of bifurcations leading to a basin fractalization is the guideline. As for the nonfractal basins, these bifurcations are characterized by a common feature: *the contact of the basin boundary with the critical set LC*. Even if the structure of LC is simple, the basin boundary may be very complex with a large variety of geometrical situations, which leads to a large variety of contact bifurcations and fractalization of the boundaries.

The basins generated by two-dimensional noninvertible maps may be either *simply connected*, or *multiply connected*, or *nonconnected*, depending on the position of their boundary with respect to the critical set LC [Mira *et al.*, 1996a; Mira *et al.*, 1996b]. We remind that a basin is multiply connected when it is pierced by holes, called *lakes* in the above references, and for a (Z_1–Z_3–Z_1) map these holes are necessarily infinitely many, because each of them has infinitely many preimages. Analogously, when a basin of a (Z_1–Z_3–Z_1) is nonconnected, it is always made up of infinitely many areas (called *islands*) without any connection, contrarily to (Z_0–Z_2) maps which may have only one island in the Z_0 area in certain cases. For the maps (1) here considered, the limit set of lakes, or islands, may include a finite number of cycles, or infinitely many cycles, or invariant manifolds of saddle cycles, or repelling invariant closed curves, or *strange repellers* (*SR* henceforth) resulting from the destabilization of chaotic attractors. In this last case the basin may have a fractal structure. In general, when the limit set of lakes or islands that constitute a basin include an invariant set on which the dynamics are chaotic, one can say that the basin has a fractal structure. We can also say that the limit set includes a strange repeller, formed by infinitely many unstable cycles of any period, unstable sets of saddle cycles, the limit set of their preimages when the period tends toward infinity, and the preimages of any rank of all these points.

As a repulsive set, a strange repeller belongs to some basin boundaries [Mira *et al.*, 1996a]. Its unstable cycles and the limit sets of their preimages come from some former chaotic attractor. When generated by noninvertible maps, a strange repeller *SR* gives rise either to *chaotic transients* toward an attractor, or to a *fractal basin*. In the first case the *SR* points are not limit points of lakes, or islands, but are located inside the area bounded by the "external" boundary of a simply connected immediate basin, where *immediate basin* means the connected portion of the basin that contains the attractor. The *SR* points belong to the total basin boundary. An initial point belonging to a small neighborhood of a *SR* generates an orbit which has an erratic behavior during a certain number of iterations, then convergence toward the attractor inside its immediate basin is observed. In the second case the *SR* points are limit points of lakes (for multiply connected basins), or islands (for nonconnected basins). Then a *SR* may be the *nucleus* of the corresponding fractal basin, as it may correspond to a *fuzzy basin boundary* separating the basins of two, or more, attractors. A simply connected basin with chaotic transients (i.e. including a *SR*) may have not a fractal structure, but it may have a

fractal boundary, because the *SR* which is at the origin of the chaotic transient belongs to the basin boundary.

About the situations giving rise to unstable fractal sets *SR*, the paper shows and explains some bifurcations leading to a qualitative change of a fractal basin generated by the map (1). More particularly:

(a) the transition from a simply connected basin, containing a *SR* set, to a fractal multiply connected basin,
(b) the transition from a fractal basin, associated with a given nucleus SR_1, to a fractal basin associated with two strange repellers SR_1 and SR_2,
(c) the transition from a fractal multiply connected basin to a fractal nonconnected basin.

All these bifurcations, as the ones related with basins without a fractal structure, are due to contacts between the critical set *LC* and a basin boundary (stable set of saddle cycle). Each of these bifurcations leads to a contact occurring in a different way with respect to the others. In general, they are of homoclinic type.

We follow the terminology of Mira *et al.* [1996a], Mira *et al.* [1996b], where the structure of the basins is described by using geographic analogies: *sea* and *continent* denote two different basins separated by a common boundary, for example, *sea* may denote the basin of divergent trajectories and *continent* the basin of bounded ones, and consequently *lakes* and *islands* denote the nonconnected portions of the sea and the continent, respectively. The term is used *roadstead* when a "lake" communicates with the "sea".

Section 2 is devoted to some reminders about general properties of two-dimensional noninvertible maps, the conditions of existence of a nonconnected basin, those related to a multiply connected basin, and also homoclinic and heteroclinic situations. Section 3 establishes the equation of the critical set. Section 4 concerns nonconnected basins and multiply connected ones with a nonfractal structure. Section 5 deals with such basins, but with fractal structure. The bifurcations denoted above as (a)–(c) are fully explained. Section 6 concludes, and indicates some consequences of the results on some extended problems for which two-dimensional noninvertible maps play a role.

2. Some Reminders

2.1. *General properties*

Consider a continuous two-dimensional noninvertible map T, i.e. such that the highest degree k of a region Z_k is $k \geq 2$. Whether T be smooth or not, the rank-one critical curve *LC* is defined as the locus of points such that at least two determinations of the inverse correspondence are merging. In general, a critical curve *LC* is made up of several branches. The locus of these "coincident first rank preimages" is a curve LC_{-1}, called *curve of merging preimages*. As in any neighborhood of a point of *LC* there are points for which at least two distinct inverses are defined, LC_{-1} is a set of points for which the Jacobian determinant of T vanishes if T is smooth, or for which the noninvertible map T is not differentiable. The curve *LC* satisfies the relations $T(LC_{-1}) = LC$, and $T^{-1}(LC) \supseteq LC_{-1}$.

The simplest case is that of maps in which *LC* (made up of only one branch) separates the plane into two open regions Z_0 and Z_2. A point $X(x, y)$ belonging to Z_2 has two distinct preimages (or antecedents) of rank one, and a point X of Z_0 has no real preimages. The corresponding maps are said to be of (Z_0–Z_2) type. In more complex cases a classification of noninvertible maps from the structure of the set of Z_k regions can be made [Mira *et al.*, 1996a]. It is worth noting that with two-dimensional noninvertible maps the organization of bifurcations, for example in a parameter plane, may be very different from that given by invertible maps

A closed and invariant set A is called an *attracting set* if some neighborhood U of A exists such that $T(U) \subset U$, and $T^n(X) \to A$ as $n \to \infty$, $\forall X \in U$. An attracting set A may contain one, or several attractors. It may coexist with sets of repulsive points (strange repellers) giving rise to either *chaotic transients* towards these attractors, or *fuzzy boundaries* of their basin [Mira, 1987; Mira *et al.*, 1996]. The open set $D = \bigcup_{n\geq 0} T^{-n}(U)$ is the total basin of A, i.e. D is the open set of points X whose forward trajectories (set of increasing rank images of X, or orbits) converge towards A. For the map (1) the basin D is invariant under backward iteration T^{-1} of T, but not necessarily invariant by T

$$T^{-1}(D) = D, \qquad T(D) \subseteq D$$

For the boundaries ∂D in general the following relations hold

$$T^{-1}(\partial D) \supseteq \partial D, \qquad T(\partial D) \subseteq \partial D$$

The strict inclusions $\subset$ hold iff D contains points of a Z_0 region, whereas the strict inclusion $\supset$ occurs only for particular classes of maps. For the family (1) the equality holds in all the relations given above.

If A is a connected attractor (simplest case: A is a fixed point), the *immediate basin* D_0 of A, is defined as the widest connected component of D containing A.

We remark that $T^{-1}(\partial D) = \partial D$ implies that ∂D must contain the set of preimages of any of its cycles, i.e. must contain the stable set W^s of any cycle of T belonging to ∂D, while $T(\partial D) \subseteq \partial D$ means that the images of any of its points belongs to $\partial D \cap Z_k$, $k \geq 1$. For unstable node and focus cycles, it is worth noting that the stable set W^s is made up of the set of increasing rank preimages of cycle points (such a set does not exist in the case of an invertible map). For a saddle cycle, W^s is made up of the local stable set W^s_l, associated with the determination of the inverse map for which this cycle is invariant, and its preimages of any rank.

When A is the widest attracting set of a map T, its basin D (called *continent* in [Mira *et al.*, 1994] and [Mira *et al.*, 1996a]) is the open set D containing A such that its closure $\overline{D}$ is the locus of points of the plane having bounded trajectories. Its complementary set, denoted by D' (i.e. $\overline{D} \cup D' = \mathbf{R}^2$) when it is nonvoid, is the basin (called *sea* in [Mira *et al.*, 1996a]) of an attracting set at infinity (on the Poincaré's equator), i.e. the locus of points of the plane having divergent trajectories. In such a case the two basins have a common boundary (the separating set).

A map T may also possess no attracting set at finite distance (when only repellers, chaotic or not, exist at finite distance). In such a case, the locus of points of the plane having bounded trajectories belongs to the boundary $\partial D'$ of D' (and $\mathbf{R}^2 = \overline{D'}$). Then $\partial D'$ may be a strange repeller giving rise to a chaotic transient toward the Poincaré's equator.

2.2. *Existence of a nonconnected basin, and a multiply connected basin. Their bifurcations*

In the case of a (Z_0–Z_2) map we have $T^{-1}(LC) = LC_{-1}$, see e.g. [Mira *et al.*, 1996a; Mira *et al.*, 1996b]. Instead, a (Z_1–Z_3–Z_1) map is characterized by $T^{-1}(LC) \supset LC_{-1}$. In this case the inverse of LC generates an *extra-preimage*, denoted by $\overline{LC}_{-1}$, such that $T^{-1}(LC) = LC_{-1} \cup \overline{LC}_{-1}$ [Mira *et al.*, 1996a], where $LC_{-1} = L_{-1} \cup L'_{-1}$ and $\overline{LC}_{-1} = \overline{L}_{-1} \cup \overline{L}'_{-1}$.

Before showing the numerical explorations of the rich dynamic scenarios of the family of maps (1) along some bifurcation paths in the space of parameters, we now show some qualitative pictures to explain exemplary situations leading to contact bifurcations that change the topological structure of the basins of attraction in a (Z_1–Z_3–Z_1). Figures 1 and 2 describe the situations leading to a nonconnected basin, and a multiply connected basin. If $X(x, y) \in Z_3$ the inverse map has three determinations $T^{-1}(X) = T_1^{-1}(X) \cup T_2^{-1}(X) \cup T_3^{-1}(X)$. If $X \in LC$, then $T_1^{-1}(X) = T_2^{-1}(X) \in LC_{-1}$. If $X \in LC$, then $T^{-1}(X) = X_{-1}^{1\text{-}2} \cup X_{-1}^{3}$ with $X_{-1}^{1\text{-}2} \in LC_{-1}$. In this text, the symbolisms $X_{-1}^{1\text{-}2}$, $D_n^{1\text{-}2}$, $H_n^{1\text{-}2}$ respectively indicate that a point X belongs to LC_{-1}, a rank-n island and a rank-n lake [Mira *et al.*, 1994; Mira *et al.*, 1996a] are crossed by LC_{-1}.

Figure 1(a) corresponds to a nonconnected basin D of an attracting set A (a fixed point P in the figure). Let D_0 be the immediate basin of A. The basin D is nonconnected because $D_0 \cap \overline{Z}_3$ is nonconnected, and $\Delta_0 \subset D_0 \cap Z_3$ (Δ_0 is called *headland*) does not contain A. The three rank-one inverses of Δ_0 are given by $T^{-1}(\Delta_0) = T_1^{-1}(\Delta_0) \cup T_2^{-1}(\Delta_0) \cup T_3^{-1}(\Delta_0)$, $T_1^{-1}(\Delta_0) \cup T_2^{-1}(\Delta_0) = D_1^{1\text{-}2}$, $T_3^{-1}(\Delta_0) = D_1^3$. In this figure the islands (nonconnected parts of the basin) $D_1^{1\text{-}2}$ and D_1^3 belonging to Z_1, they have only one rank-one preimage $D_2^{1\text{-}2}$ and D_2^3. If these islands, or one of their preimages, belong to Z_3, then it gives rise to three preimages, and this process may lead to an arborescent sequences of islands. In any case, for maps of type (Z_1–Z_3–Z_1), each island has at least one preimage, so an infinite sequence of preimages always exist.

Noninvertible maps with an area Z_k, $k > 2$, can generate islands without the presence of a headland, as represented in Fig. 1(b). This occurs when the immediate basin D_0 of the stable fixed point P is such that $\partial D_0 \cap L = \emptyset$, $\partial D_0 \cap L' \neq \emptyset$ (or conversely). Let $B_0 = D_0 \cap Z_3$, with $T^{-1}(B_0) = T_1^{-1}(B_0) \cup T_2^{-1}(B_0) \cup T_3^{-1}(B_0)$. As shown from the positions of the points a, b, and their rank-one preimages, $T_1^{-1}(B_0) \cup T_2^{-1}(B_0) = D_0$, and $T_3^{-1}(D_0)$ belongs to the island D_1, as $T_3^{-1}(B_0)$ is part of D_1 on the left of $\overline{L}'_{-1}$. The rank-one inverses of P are given by $T_1^{-1}(P) = P$, $T_2^{-1}(P) = P_{-1}$, $T_3^{-1}(P) = P'_{-1}$. The island D_1 belonging to Z_1 has only a rank-one preimage D_2. Let $B_2 = D_2 \cap Z_3$ due to $D_2 \cap Z_3 \neq \emptyset$,

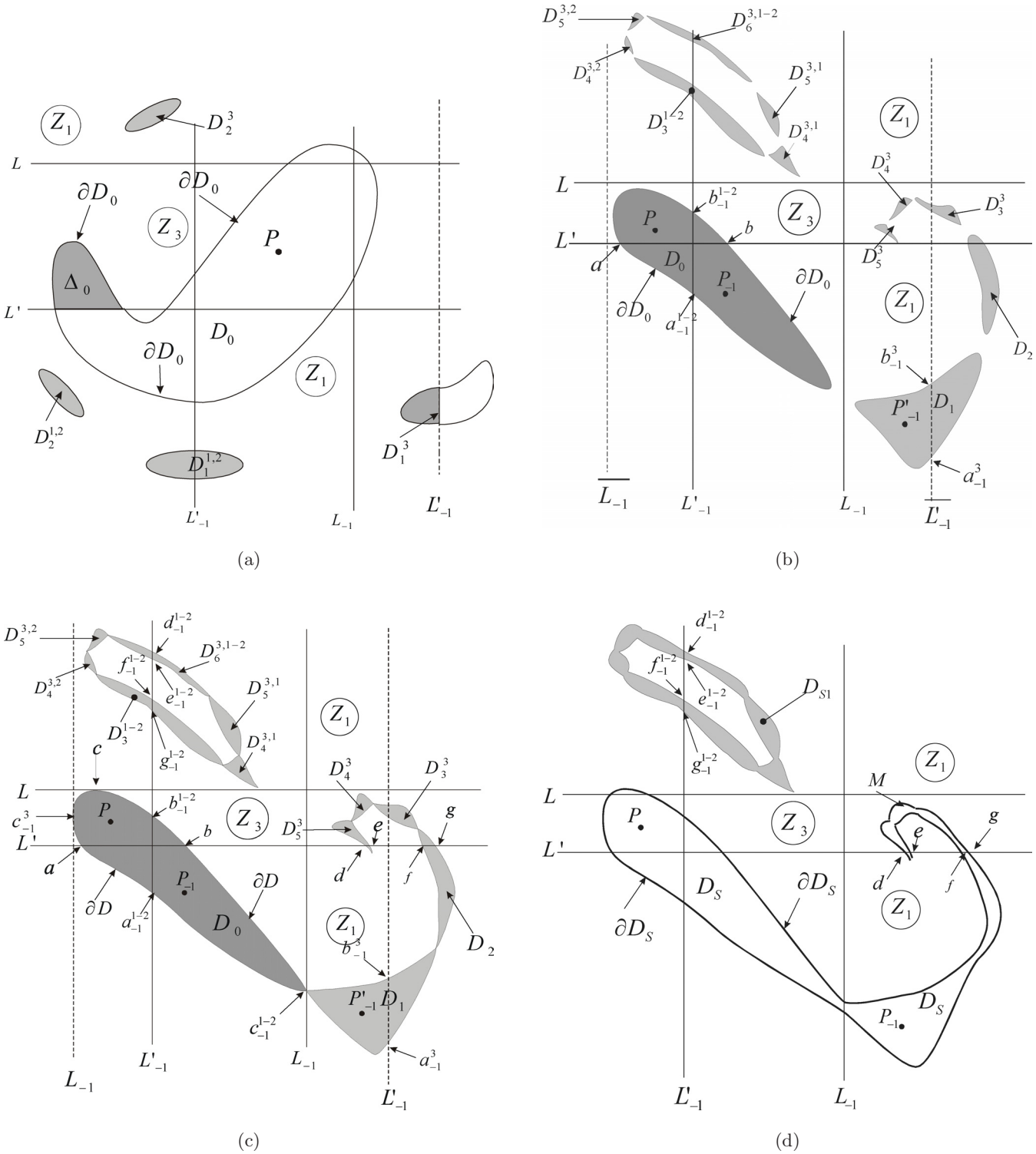

Fig. 1. (a) Nonconnected basin D of the fixed point P. Let D_0 be the immediate basin of P. The three rank-one inverses of the headland Δ_0 are the islands (nonconnected parts of the basin) given by $T^{-1}(\Delta_0) = T_1^{-1}(\Delta_0) \cup T_2^{-1}(\Delta_0) \cup T_3^{-1}(\Delta_0)$, with $T_1^{-1}(\Delta_0) \cup T_2^{-1}(\Delta_0) = D_1^{1-2}$, $T_3^{-1}(\Delta_0) = D_1^3$. (b) Islands generated without a headland presence. The immediate basin D_0 of the stable fixed point P is such that $\partial D_0 \cap L = \emptyset$, $\partial D_0 \cap L' \neq \emptyset$. (c) A global bifurcation happens when ∂D_0 has a tangential contact with L at the point c. It results from a tangential contact of ∂D_0 with the extra-preimage $\overline{L}_{-1}$ at the point $c_{-1}^3 = T_3^{-1}(c)$ and a nontangential contact with L_{-1} at the point $c_{-1}^{1-2} = T_1^{-1}(c) = T_2^{-1}(c)$, angular contact point of D_0 with D_1. (d) After the bifurcation, a connection of an island subset with the immediate basin D_0 occurs. A larger immediate basin D_S results, with aggregation of some island sets nonconnected with D_S, such as the preimages of $B_S = D_S \cap Z_3$.

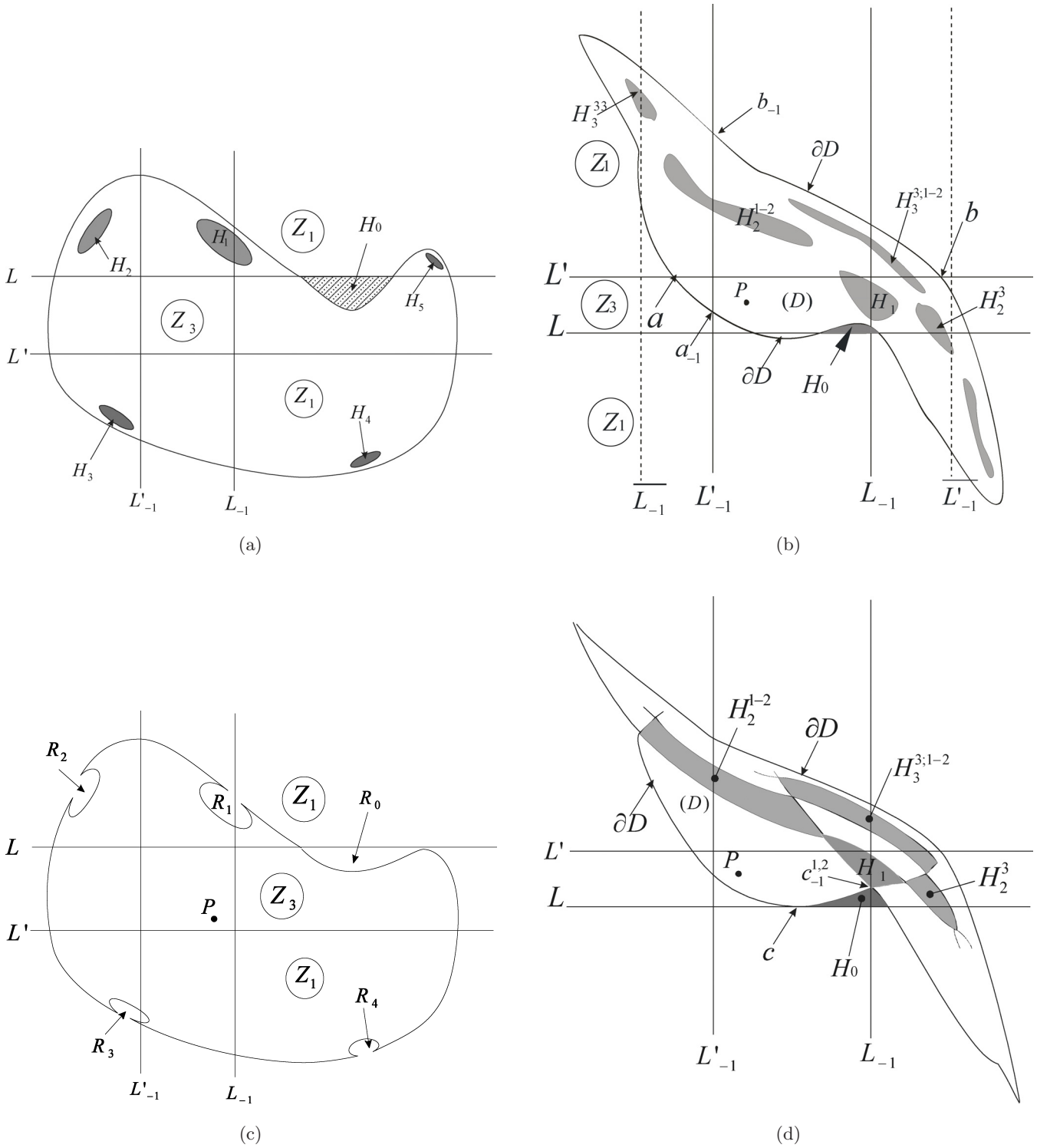

Fig. 2. (a) Multiply connected basin D of the stable fixed point P. The hatched area H_0 is called a *bay*, the holes $H_n = T^{-n}(H_0)$, $n = 1, 2, 3, \ldots$, are called *lakes*. The rank-one lake is given by $H_1 = T_1^{-1}(H_0) \cup T_2^{-1}(H_0)$. The lakes H_n, remaining in the Z_3 region, do not form an arborescent sequence when $n \to \infty$. (b) The lakes H_n form an arborescent sequence. Indeed H_1 intersects Z_3 and L', as some of its increasing rank preimages. (c) Bifurcation from Fig. 2(a) when the boundary ∂D has a contact with the critical arc L. This leads to an opening of the *lakes* in the *sea* (domain of divergent orbits), with creation of *roadsteads* R_n, $n = 1, 2, 3, \ldots$. (d) Bifurcation from Fig. 2(b), leading to a direct bifurcation *multiply connected basin* $\leftrightarrows$ *nonconnected basin*. The point c is the contact point between ∂D and L, $c_{-1}^{1-2} = T_1^{-1}(c) = T_2^{-1}(c) \in L_{-1}$ being an angular contact point between H_0 and H_1. (e) After the bifurcation the basin D is nonconnected, made up of arborescent sequences of islands $T_0^{-n}(D_0)$.

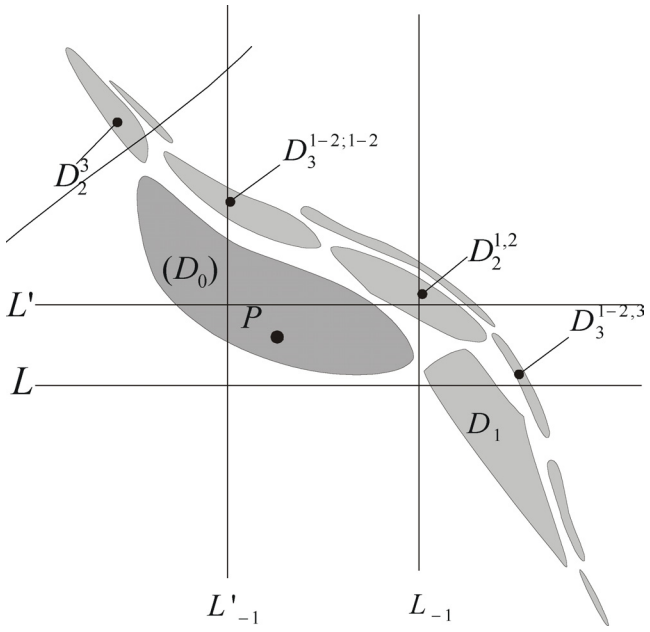

(e)

Fig. 2. (*Continued*)

$D_2 \cap L' \neq \emptyset$, one has $T^{-1}(D_2) = D_3^{1-2} \cup D_3^3$, with $D_3^{1-2} = T_1^{-1}(B_2) \cup T_2^{-1}(B_2)$, island crossed by L'_{-1}, $D_3^3 = T_3^{-1}(D_2)$, island crossed by $\overline{L}'_{-1}$. The islands are obtained in an equivalent way, and are infinitely many.[1] A global bifurcation happens when ∂D_0 has a tangential contact with the critical segment L at the point c [Fig. 1(c)]. Consequently, a tangential contact occurs between ∂D_0 and the extra-preimage $\overline{L}_{-1}$ at the point $c_{-1}^3 = T_3^{-1}(c)$ and a nontangential contact with L_{-1} at the point $c_{-1}^{1-2} = T_1^{-1}(c) = T_2^{-1}(c)$, which is an angular contact point of D_0 with D_1. This situation leads to an aggregation of a islands subset with the immediate basin D_0, as indicated in Fig. 1(c). A larger immediate basin D_S results, with aggregation of some islands sets nonconnected with D_S, such as the first one $D_{S1} = T_1^{-1}(B_S) \cup T_2^{-1}(B_S)$, $B_S = D_S \cap Z_3$, which has an annular aspect due to $\partial D_S \cap L' = d \cup e \cup f \cup g \neq \emptyset$. If a basin intersects simultaneously the two branches L and L' of LC, then the basin becomes simply connected. This would have been the case if, instead of having a local maximum M of ordinate in Z_3 [Fig. 1(d)], ∂D_S would have intersect L.

Figure 2(a) corresponds to a multiply connected basin D of an attracting set A (here a stable fixed point P). Let D^* be the simply connected region obtained by eliminating all the holes of D. D is multiply connected because $T^{-1}(D^*) \subset D^*$, $T(D^* \cap LC_{-1}) \supset D^* \cap LC$. The hatched area H_0 is called a *bay*, $H_n = T^{-n}(H_0)$, $n = 1, 2, 3, \ldots$, are holes (*lakes*) inside D^*. The first lake $H_1 = T_1^{-1}(H_0) \cup T_2^{-1}(H_0)$ intersects L_{-1}, and is generated by the bay. The third inverse $T_3^{-1}(H_0)$ does not generate a hole. The lakes of Fig. 2(a) belong to Z_1, and so the lakes H_n (although infinitely many) do not form an arborescent sequence when $n \to \infty$. In Fig. 2(b) for which H_1 intersects Z_3 and L', as some of its increasing rank preimages. Then $T^{-1}(H_1) = T_1^{-1}(H_1) \cup T_2^{-1}(H_1) \cup T_3^{-1}(H_1)$, with $T_1^{-1}(H_1) \cup T_2^{-1}(H_1) = H_2^{1-2}$ intersecting L'_{-1}, $T_3^{-1}(H_1) = H_2^3$ intersecting $\overline{L}'_{-1}$, $H_3^{3;2-1} = T_1^{-1}(H_2^3) \cup T_2^{-1}(H_2^3)$ intersecting L_{-1}, etc. We may have a finite number of lakes belonging to Z_3 or infinitely many, and only in the latter case the lakes form an arborescent sequence.[2]

Figure 2(a) shows a multiply connected basin that undergoes a bifurcation when ∂D^* has a contact with the critical arc L which leads to an opening of the *lakes* in the *sea* (domain of divergent orbits), with creation of *roadsteads* R_n, $n = 1, 2, 3, \ldots$ [Fig. 2(c)]. Thus Fig. 2(c) shows the

[1]Only a few of them are represented in the qualitative figures.

[2]In fact, even if a point belonging to Z_3 has three preimages, such preimages may all belong to Z_1.

bifurcation *multiply connected basin* $\leftrightarrows$ *simply connected basin*. The same type of contact of Fig. 2(b), with infinitely many sequences of lakes, may lead to a direct bifurcation *multiply connected basin* $\leftrightarrows$ *nonconnected basin*. This bifurcation corresponds to Fig. 2(d), where c is the contact point between $\partial D \equiv \partial D^*$ and L, $c_{-1}^{1-2} = T_1^{-1}(c) = T_2^{-1}(c) \in L_{-1}$ being an angular contact point between H_0 and H_1. After the bifurcation the basin D is nonconnected, made up of infinitely many sequences of islands $T_0^{-n}(D_0)$ [Fig. 2(e)].

2.3. *Homoclinic and heteroclinic situations*

Let U be a neighborhood of an unstable fixed point (saddle, node or focus) p^*. The *local* (i.e. in U) *unstable set* of p^* is defined as the locus of points in U having a sequence of preimages in U which tend toward $p*$. The *global unstable set* is the locus of all points of the domain having a sequence of preimages that converge toward p^*, and can be obtained by constructing the images of the local unstable set. When the map T is continuous and noninvertible, the invariant unstable set $W^u(p^*)$ of a saddle point p^* is connected and self-intersections may occur (so that it may not be a manifold). This cannot happen for invertible maps. Self-intersections and loops of $W^u(p^*)$ are described in [Gumowski & Mira, 1980a, pp. 373–374; Gumowski & Mira, 1980b, pp. 203–222; Mira *et al.*, 1996a, pp. 506–515]. The role of critical curves and curves of merging preimages is again essential in the understanding of the formation of self-intersections of the unstable set of a saddle fixed point.

The *stable set* $W^s(p^*)$ of a saddle p^* is backward invariant, $T^{-1}[W^s(p^*)] = W^s(p^*)$, and it is mapped onto itself by T, $T[W^s(p^*)] \subseteq W^s(p^*)$. The stable set is invariant if T is invertible, while for a noninvertible map it may be strictly mapped onto itself. When T is continuous, self-intersections cannot occur (so that it may be called manifold, being a connected manifold, or the union of disjoint connected components which are manifolds). When T is noninvertible, $W^s(p^*)$ *may be nonconnected and made up of infinitely many closed curves*, passing through the increasing rank preimages of p^*. An equivalent property holds for higher dimensions.

While in invertible maps an expanding fixed point (unstable node, or focus) p^* has no stable set, when T is noninvertible the stable set of p^* is given by all the preimages (of any rank) of this point: $W^s(p^*) = \bigcup_{n\geq 0} T^{-n}(p^*)$.

A point q is said to be *homoclinic* to the nonattracting fixed point p^* (or homoclinic point of p^*) iff $q \in W^s(p^*) \cap W^u(p^*)$. *Heteroclinic points* are obtained when the stable and unstable sets are related to two different fixed points. A "contact bifurcation" (between a critical set and a stable (or unstable) set) may correspond to homoclinic and heteroclinic bifurcations, and critical curves are useful for interpreting such problems, and the related bifurcations. Classically homoclinic and heteroclinic situations are defined for n-dimensional diffeomorphisms, for $n > 1$, only for saddle points. It is worth noting that the first "extended" notion (with respect to the classical one) of homoclinic and heteroclinic points in one-dimensional noninvertible maps, with indication of its generalization for m-dimensional maps, $m > 1$, was introduced by Sharkovsky [1969].

2.4. *The problem of numerical simulations*

Numerical simulations are used to obtain the results of the paper, in particular, to obtain a delimitation of the basins and to discuss their bifurcations. Based on finite precision of computer calculations, such a method gives only a *macroscopic view* of the map behavior, and consequently it requires a critical analysis of the results. Considering the *microscopic point of view*, it is worth to note that in 1979 Newhouse formulated a very important theorem. It states that in any neighborhood of a C^r-smooth ($r \geq 2$) dynamical system, there exist regions of the space of dynamical systems (or a parameter space) for which systems with homoclinic tangencies (with structurally unstable, or nonrough homoclinic orbits) are dense. Domains having this property are called *Newhouse regions*. This result was completed by V. S. Gonchenko, D. V. Turaev and L. P. Shilnikov who assert that systems with infinitely many homoclinic orbits of any order of tangency, and with infinitely many arbitrarily degenerate periodic orbits, are dense in the Newhouse regions of the space of dynamical systems (cf. [Shilnikov, 1997]). This fact has an important consequence: *systems belonging to a Newhouse region are such that a complete study of their dynamics and bifurcations is impossible*. Indeed in many smooth cases, due to the finite time of a simulation, what appears numerically as

a chaotic (strange) attractor may contain a "large" hyperbolic subset in presence of a finite or an infinite number of stable periodic solutions. Generally such stable solutions have high periods, and narrow "oscillating" tangled basins, which are impossible to exhibit numerically due to the finite time of observation, and unavoidable numerical errors. So it is only possible to consider some of the characteristic properties of the system, their interest depending on the nature of the problem. Such complex behaviors occur for p-dimensional flows, $p > 2$, and thus for $p \geq 2$ invertible and noninvertible maps.

From a *macroscopic point of view* (the one considered in this paper) the union of the numerous, and even infinitely many stable solutions, which are stable cycles for a map, forms an attracting set denoted by A. A numerical simulation, by definition, is made of a limited number of iterations. Consider the case of a noninvertible map giving rise to a chaotic attractor, and the elimination of a transient, made up of a sufficiently large set of "initial" iterations. Then either the numerical simulation reproduces points of the chaotic area, related to a "strict" strange attractor in the mathematical sense, or represents a transient toward an attracting set A including stable cycles of large periods. The first case for example is that of some piecewise smooth maps (i.e. with points of nonsmoothness), not permitting stable cycles (i.e. the Jacobian determinant cannot be sufficiently small). In the second case, supposing numerical iterations without error, the transient would be toward a stable cycle having a period larger than the number of iterations, this transient occurring inside a very narrow basin, intermingled with similar basins of the other stable cycles of large period. In the presence of unavoidable numerical errors, the iterated points cannot remain inside the same narrow basin. They sweep across the narrow tangled basins of cycles of the attracting set A. Then they reproduce a chaotic area bounded by segments of critical curves of increasing rank until a certain rank (see e.g. [Mira, 1987]). This means that the boundary of the chaotic area is the one observed numerically, in the smooth case as a transient toward an attracting set located inside the area, in the nonsmooth case as the boundary of a strange attractor. Such a property constitutes an important characteristic of the system dynamics. This shows the interest of the notion of chaotic area bounded by critical arcs (cf. [Mira *et al.*, 1996a]), even if in the smooth case it is impossible to discriminate numerically a situation of a strange attractor in the mathematical sense, from that of an attracting set made up of stable cycles with very large period.

3. Determination of the Critical Sets

The map (1) has three fixed points $O = (0; 0)$, $P = (x_P, y_P)$ and $Q = (x_Q, y_Q)$, where

$$x_P = \frac{-b + \sqrt{b^2 - 4ac}}{2c},$$

$$x_Q = \frac{-b - \sqrt{b^2 - 4ac}}{2c}$$

$$y_P = y_Q = 0$$

In the following, the multipliers (eigenvalues) of the Jacobian matrix of T, evaluated at the fixed points, will be denoted by S_1 and S_2.

The inverses of T are given by the solutions of the cubic equation

$$cx^3 + bx^2 + (a - d)x + dx' - y = 0, \quad y = x' - x \tag{2}$$

For $d = -1$ the map T^2, obtained after two iterations, turns into a map with separated variables (x, $u = x + y$)

$$\begin{aligned} x'' &= ax + bx^2 + cx^3 \\ u'' &= au + bu^2 + cu^3 \end{aligned} \tag{3}$$

The boundaries of the regions Z_k, $k = 1, 3$, are made up of two parallel straight lines L, L', branches of the rank-one critical curve $LC = L \cup L'$.

The set LC, defined as the locus of points such that two determinations of the inverse map T^{-1} are merging on the set $LC_{-1} = L_{-1} \cup L'_{-1}$, is given by $LC = T(LC_{-1}) = T(L_{-1}) \cup T(L'_{-1})$, where the two branches of LC_{-1} can be obtained by equating to zero the Jacobian determinant of T, i.e.:

$$\begin{aligned} L_{-1} &: x = \frac{-b + \sqrt{b^2 - 3c(a - d)}}{3c} = \alpha_+, \\ L'_{-1} &: x = \frac{-b - \sqrt{b^2 - 3c(a - d)}}{3c} = \alpha_- \end{aligned} \tag{4}$$

The extra-preimages $\overline{L}_{-1}$ and $\overline{L}'_{-1}$ are defined from (2) taking into account (4). Put $f(x) \equiv ax + bx^2 + cx^3$, then

$$\begin{aligned} L &: y = f(\alpha_+) + d(x - \alpha_+), \\ L' &: y = f(\alpha_-) + d(x - \alpha_-) \end{aligned} \tag{5}$$

4. Nonconnected and Multiply Connected Basins with a Nonfractal Structure

4.1. *Transition simply connected basin ↔ multiply connected basin*

Consider (1) and the parameter set $a = c = 1$, $d = 0$, $-2.4 \leq b < -2.6$. The fixed point O is a saddle ($-1 < S_1 < 0$, $S_2 > 1$), the points P and Q are respectively a stable focus denoted by F in Fig. 3, and an unstable node ($S_1 < -1$, $S_2 > 1$) denoted by N_1 in Fig. 3. For the set of parameters considered here, the map T generates two cycles of period two: a saddle C_2^j and an unstable node N_2^j, $j = 1, 2$.

We start our numerical explorations from $b = -2.4$, a parameter situation that gives a simply connected basin D of the stable fixed point F, represented by the brown region in Fig. 3. For $b = b_{f0} \simeq -2.4228$ the basin D becomes multiply connected, due to the creation of a bay H_0 in the region Z_3 after a contact bifurcation between L' and the basin boundary ∂D (see Fig. 4, obtained for $b = -2.43$).

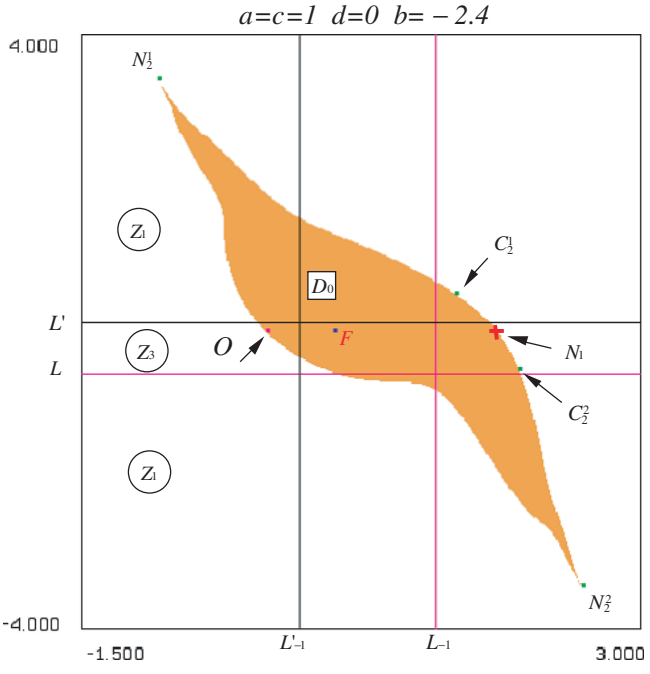

Fig. 3. Map T with $a = c = 1$, $b = -2.4$, $d = 0$. The fixed point C_1 is a saddle ($-1 < S_1 < 0$, $S_2 > 1$). F is a stable focus, denoted F, N_1 an unstable node ($S_1 < -1$, $S_2 > 1$) denoted N_1. The map T generates two period two cycles: a saddle C_2^j and an unstable node N_2^j, $j = 1, 2$. The basin D of F is simply connected.

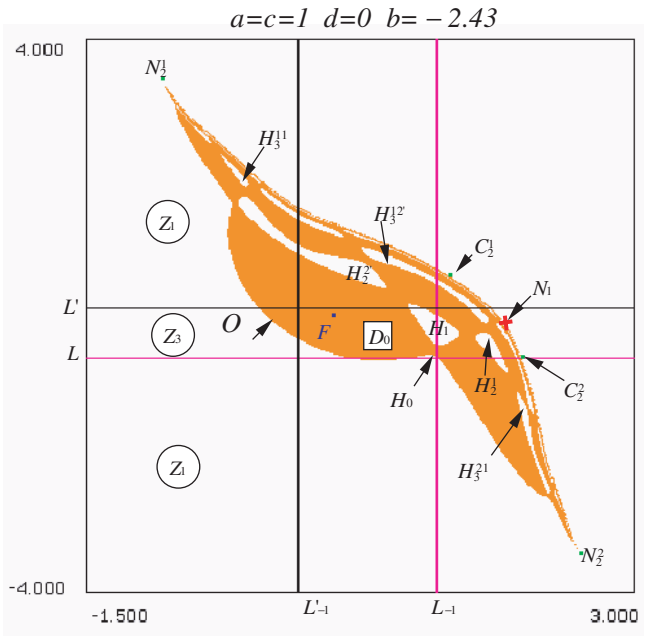

Fig. 4. Map T with $a = c = 1$, $b = -2.43$, $d = 0$. Situation after the bifurcation $b = b_{f0} \simeq -2.4228$, a contact bifurcation between L' and the basin boundary ∂D at a local maximum of the ∂D ordinate. The basin D becomes multiply connected by creation of a bay H_0.

The rank-one lake is $H_1 = T^{-1}(H_0)$, made up of the union of two preimages joining across L_{-1}. The third preimage of ∂H_0 gives an arc of ∂D, according to the qualitative situation described in Fig. 2(b). The rank-$(n+1)$ lakes $T^{-n}(H_1) = H_{n+1}^{i_1 \cdots i_n}$, $n = 1, 2, \ldots$, form an incomplete arborescent sequences when $n \to \infty$, in the sense that only one rank-n lake has a part belonging to Z_3. Recall that every point of Z_3 has three rank-1, that may all belong to Z_3, or only two of them, the third one being in Z_1, or only one or zero, i.e. all the three preimages may belong to Z_1. In the situation represented in Fig. 4 we have that one branch of the increasing rank iteration tree has three preimages, the two other branches have only one preimage. This results in that the sequence of lakes cannot create a fractal structure. The limit set of this sequence is an arc of curve made up of the stable manifold of the period two saddle C_2^j, $j = 1, 2$, which includes the repelling node N_1, bounded by the period two unstable node N_2^j, $j = 1, 2$, belonging to Z_1, as shown in Fig. 4.

The contact bifurcation occurring at $b = b_{f0}$ changes the simply connected basin D into a nonfractal multiply connected one, pierced with holes that have an arc of the stable manifold of a period two saddle as limit set.

4.2. *Direct transition nonconnected basin ↔ multiply connected basin*

For $b = b_{f1} \simeq -2.4317$ a contact bifurcation between L' and the basin boundary ∂D occurs at the point B shown in Fig. 5 (compare also with the situation qualitatively represented in Fig. 2(d)). Then for $b_{f1} < b < 2.6$, the basin D of the stable focus F becomes nonconnected. Let D_0 be its immediate basin, $D_1 = T^{-1}(D_0)$ the rank-one island. It is worth to note that the island D_1, $\partial D_1 \cap L' \neq \emptyset$, is not created here from an headland, but according to the situation described in Fig. 1(b). In this example, at each iteration only one island has a part inside Z_3. As above for the lakes, the rank-$(n+1)$ islands $T^{-n}(D_1) = D_{n+1}^{i_1 \cdots i_n}$, $n = 1, 2, \ldots$, form an incomplete arborescent sequences when $n \to \infty$, in the sense that only one rank-n island has a part belonging to Z_3. The limit set of this sequence is the arc of the stable manifold of the period two saddle C_2^j, $j = 1, 2$, bounded by the period two unstable node N_2^j, $j = 1, 2$, as shown in Fig. 6 ($b = -2.45$). This limit set is not fractal, hence the sequence of islands cannot create a fractal structure.

The contact bifurcation occurring $b = b_{f1}$ changes the multiply connected basin D into a

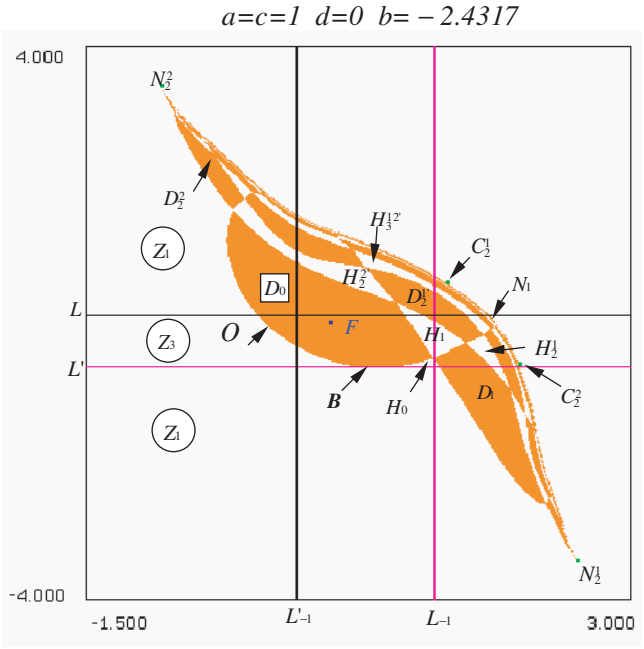

Fig. 5. Map T with $a = c = 1$, $b = b_{f1} \simeq -2.4317$, $d = 0$. A contact bifurcation between L' and the basin boundary ∂D occurs at the point b, i.e. at a local minimum of the ∂D ordinate [situation of Fig. 2(d)].

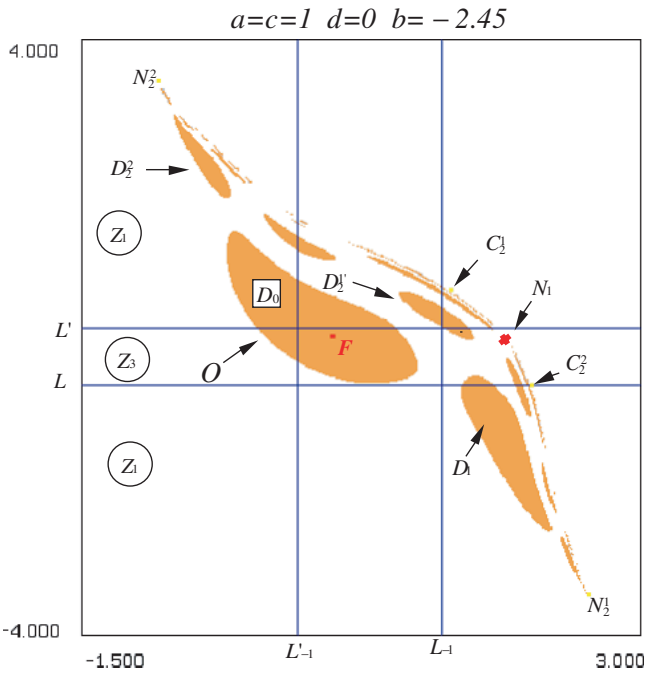

Fig. 6. Map T with $a = c = 1$, $b = -2.45$, $d = 0$. After the bifurcation $b = b_{f1}$ the basin D of the stable focus F becomes nonconnected. The rank-one island is $D_1 = T^{-1}(D_0)$, D_0 being the immediate basin of F. The contact bifurcation $b = b_{f1}$ changes the multiply connected basin D directly into a nonconnected basin with the same limit set as in Fig. 2(e).

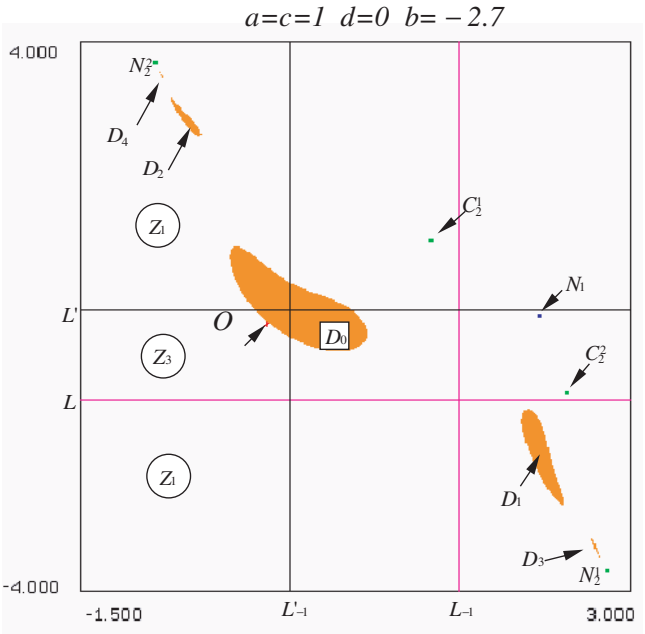

Fig. 7. Map T with $a = c = 1$, $b = -2.7$, $d = 0$. For $b = b_{f2} \simeq -2.4956$ a contact bifurcation, between L' and the island boundary ∂D_1 at the maximum ordinate of ∂D_1, has occurred. Now for $b_{f2} < b < 2.6$, $\partial D_1 \cap L' = \emptyset$, no island belongs to Z_3, all the rank-n islands belong to the regions Z_1. They form a nonarborescent sequence with the period two unstable node N_2^j, $j = 1, 2$, as limit set.

nonconnected basin with the same limit set both for the sequence of lakes and islands (see also the qualitative representation in Figs. 2(d) and 2(e)).

For $b = b_{f2} \simeq -2.4956$ a contact bifurcation, between L' and the island boundary ∂D_1, occurs. For $b_{f2} < b < 2.6$, $\partial D_1 \cap L' = \emptyset$, no island belongs to Z_3, all the rank-n islands belong to the regions Z_1. They form an infinite sequence with the period two unstable node N_2^j, $j = 1, 2$, as limit set (see Fig. 7, obtained for $b = -2.7$).

The contact bifurcation occurring at $b = b_{f2}$ changes the nonconnected basin D with an arc of saddle manifold as limit set for the islands into a nonconnected basin with two points as limit set.

We remark that in all the situations considered in this section no strange repeller exists.

5. Nonconnected and Multiply Connected Basins with a Fractal Structure

5.1. *Bifurcations in the presence of strange repellers. First situation*

5.1.1. *Origin of the strange repellers*

We now consider a bifurcation path with a fixed set of parameters $a = 0.5$, $c = -1$, $d = 0$, and increasing values of b in the interval $0.5 \le b < 1$. The fixed point O is a saddle ($-1 < S_1 < 0$, $S_2 > 1$), the fixed point P is a stable focus, and Q an unstable focus. For $b = 0.5$, the map T has two attractors; the stable focus P, and a stable invariant closed curve Γ resulting from a Neimark bifurcation after destabilization of the focus Q (Fig. 8). T also generates a period six saddle C^j with a "satellite" unstable focus F^j, $j = 1, 6$. The closure $\overline{D}$ of the basin D of the attracting set $\Gamma \cup P$ is bounded by the stable manifold of the period six saddle C^j, $j = 1, \ldots, 6$, that forms the *external boundary* $\partial_e D = \partial\overline{D}$. Let $D(P)$ and $D(\Gamma)$ be the basins of P and Γ, respectively. These two basins have a common boundary $\partial D(P) = \partial D(\Gamma)$ which includes the stable manifold $W^s(O)$ of the saddle O and the external boundary $\partial_e D$, that is $\partial D(P) = \partial D(\Gamma) = W^s(O) \cup \partial_e D$. In the situation shown in Fig. 8 they are simply connected. The stable manifold $W^s(O)$ spiralling toward ∂D_e, and on $\partial_e D$ the period six saddle C^j has turned into a period six unstable node and a sequence of period-doubling cycles. From $b = 0.5$ to $b = 0.65355$, Γ undergoes a sequence of bifurcations described in [Mira *et al.*, 1996a, pp. 515–537] (cf. also [Frouzakis *et al.*, 1997; Millérioux & Mira, 1997]), leading to an attractor $\tilde{\Gamma}$ denoted as *weakly chaotic ring* (see Fig. 9, obtained with $b = 0.6535$). For this parameter value a branch of the unstable set $W^u(O)$ of the saddle O tends to $\tilde{\Gamma}$. This branch of $W^u(O)$ presents self-intersections, the other branch ends at the stable focus P. Now the basin $D(\tilde{\Gamma})$ is multiply connected due to the bay H_0 and its increasing rank preimages $H_1 = T^{-1}(H_0)$, $H_1 = T^{-1}(H_0), \ldots, T^{-n}(H_1) = H_{n+1}^{i_1 \cdots i_n}$, $n = 1, 2, \ldots$. This means that the basin $D(P)$ is nonconnected. Then the bay H_0 of $D(\tilde{\Gamma})$ is an headland for $D(P)$, and the lakes of $D(\tilde{\Gamma})$ are islands for $D(P)$. The corresponding islands of $D(P)$, or lakes of $D(\tilde{\Gamma})$, have for limit set the unstable focus Q and its increasing rank preimages, plus the external boundary $\partial_e D$ of D. Now the stable manifold $W^s(O)$ is nonconnected (it includes the boundaries of the lakes H_n). Figure 9 shows that $W^s(O)$ is very close to $\tilde{\Gamma}$, and consequently to $W^u(O)$. Indeed, at

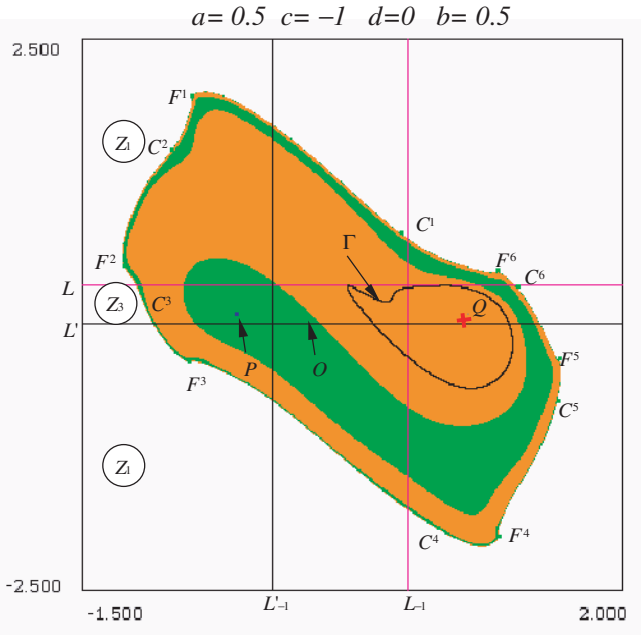

Fig. 8. Map T with $a = 0.5$, $b = 0.5$, $c = -1$, $d = 0$. The fixed point O is a saddle ($-1 < S_1 < 0$, $S_2 > 1$). The fixed point P is a stable focus, and Q an unstable focus. The map T has two attractors; the stable focus P, and a stable invariant closed curve Γ. T also generates a period six saddle C^j with a "satellite" unstable focus F^j, $j = 1, 6$. The periods of these cycles are given by colored points. The basin D of the attracting set $\Gamma \cup P$ is bounded by the stable manifold of the period six saddle C^j, $j = 1, 6$. Let $D(P)$ and $D(\Gamma)$ be respectively the basins of P and Γ, $D = D(P) \cup D(\Gamma)$. These two basins have a common boundary $\partial D(P) = \partial D(\Gamma)$ which is the stable manifold $W^s(O)$ of the saddle O, $W^s(O) = \partial D(P) = \partial D(\Gamma)$. The basins $D(P)$ and $D(\Gamma)$ are simply connected because they intersect simultaneously L and L'.

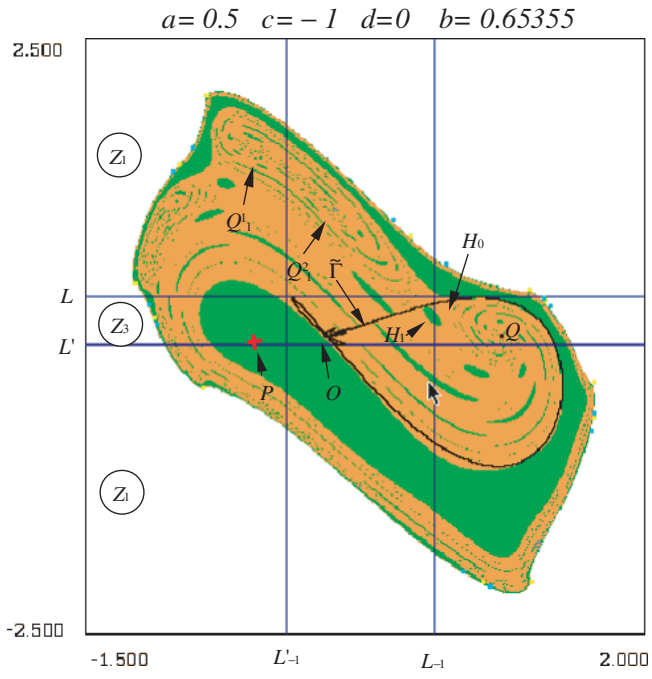

Fig. 9. Map T with $a = 0.5$, $b = 0.65355$, $c = -1$, $d = 0$. Γ has turned into an attractor $\tilde{\Gamma}$ of *weakly chaotic ring* type. For this parameter value a branch of the unstable set $W^u(O)$ of the saddle O follows $\tilde{\Gamma}$. This branch of $W^u(O)$ presents self-intersections, the other branch ends at the stable focus P. Now the basin $D(\tilde{\Gamma})$ is multiply connected due to the bay H_0 and its increasing rank preimages $H_1 = T^{-1}(H_0)$, $H_1 = T^{-1}(H_0), \ldots, T^{-n}(H_1) = H_{n+1}^{i_1 \cdots i_n}$, $n = 1, 2, \ldots$. This means that the basin $D(P)$ is nonconnected.

the value of b given by $b_{f3} \simeq 0.65355\ldots$ a tangential contact occurs between $W^s(O)$ and $W^u(O)$. This is a *homoclinic bifurcation*, leading to the destruction of $\tilde{\Gamma}$ as an attractor.

This bifurcation is associated with infinitely many unstable cycles of increasing period, that exist both for $b < b_{f_3}$ (and belong to $\tilde{\Gamma}$) and for $b > b_{f3}$, the homoclinic points being associated with cycles of period $k \to \infty$. These cycles, their stable manifolds (when they are saddles) as well as their increasing rank preimages and their limit sets, belong to a *strange repeller* SR_1 that includes the saddle O, its stable manifold $W^s(O)$ and its preimages. At a "*macroscopic scale*" (cf. Sec. 2.4) only one attractor P exists now, with basin $D(P) = D$, and $\partial D \supset SR_1$. The repulsive set SR_1 is located inside the domain bounded by the repulsive invariant closed curve $\partial_e D = \partial D \backslash SR_1$, external boundary of the basin D. A small neighborhood of SR_1 is a region whose points generate chaotic transients before converging towards P.

Important Remark. The numerical observation of the chaotic attractor $\tilde{\Gamma}$, called "weakly chaotic ring", does not imply that there are no other attractors ("microscopic" ones) out of P and $\tilde{\Gamma}$, as argued in Sec. 2.4. So, a lot of unstable cycles, among them saddles, exist in a small neighborhood of $\tilde{\Gamma}$ (see Fig. 10) giving rise to a chaotic transient toward $\tilde{\Gamma}$ (they have been numerically detected up to period 50). We consider that the strange repeller SR_1 also includes the unstable cycles such as those in Fig. 10, and their preimages of increasing rank. When we say that only one attractor P, with a basin D, exists for $b > b_{f3}$, this assertion is made in the framework of a "macroscopic" study. Indeed, this situation leads us to guess the existence of stable cycles, at least from a small parameter variation, both when an attractor $\tilde{\Gamma}$ exists and when it has disappeared leaving SR_1. Large period stable cycles with very narrow basins, tangled with similar basins of other stable cycles may exist, but they cannot be seen by numerical simulations.

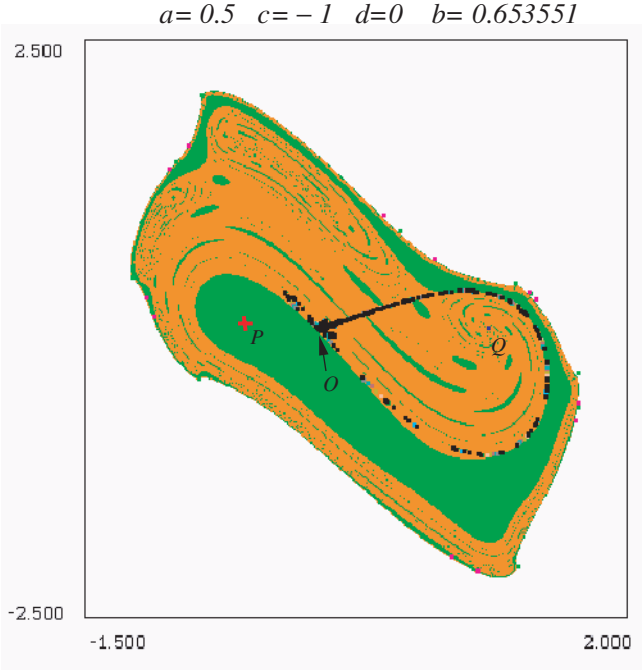

Fig. 10. Map T with $a = 0.5$, $b = 0.653551$, $c = -1$, $d = 0$. A lot of unstable cycles, among them saddles, appear in a small neighborhood of $\tilde{\Gamma}$. The periods of these cycles are given by colored points. A bifurcation value, $b_{f3} \simeq 0.653552\ldots$, gives a tangential contact between the stable set $W^s(O)$ and the unstable set $W^u(O)$ of the saddle O. This corresponds to a first homoclinic bifurcation, leading to the destruction of the attractor $\tilde{\Gamma}$ for $b > b_{f3}$, giving rise to a *strange repeller* SR_1.

5.1.2. *Basin fractalization*

Let us consider the one-dimensional map T_r, defined as the restriction of T to the repulsive invariant closed curve $\partial_e D$, $T_r = T|_{\partial_e D}$. When b is increased from $b = b_{f3}$, a sequence of period 6.2^i saddles (stable cycles of T_r on $\partial_e D$), $i = 0, 1, 2, \ldots$, turning into unstable nodes, creates a sequence of period-doubling bifurcations. For $b > b_\infty$, all these cycles turned into unstable nodes (unstable cycles of T_r on $\partial_e D$), and period $6k.2^i$ cycles, $k = 3, 4, 5, \ldots$, are created. This leads to a fractal structure of the cycles and their increasing rank preimages belonging to $\partial_e D$, constituting a new strange repeller $SR_e \in \partial_e D$. For $b = b_{f4} \simeq 0.76574$ a bay H_0 is generated via a tangential contact of $\partial_e D$ with the critical line L, at a local minimum of the ordinate of the external boundary $\partial_e D$. So the basin D becomes multiply connected (see Fig. 11, obtained for $b = 0.778$). The rank-one lake $H_1 = T^{-1}(H_0)$ is the union of two preimages of H_0. The third inverse of the boundary ∂H_0 gives an arc of the external boundary $\partial_e D$ of D. The rank-$(n+1)$ lakes $T^{-n}(H_1) = H_{n+1}^{i_1 \cdots i_n}$, $n = 1, 2, \ldots$, form an infinite arborescent sequences when $n \to \infty$. The limit set of the lakes $H_{n+1}^{i_1 \cdots i_n}$ is essentially made up of the boundary $\partial_e D$, on which the restriction of the map has a fractal structure, and a set of cycles which may be associated with homoclinic points of $W^s(O) \cap W^u(O)$ (a branch of $W^s(O)$ tends toward the external boundary $\partial_e D$ spiraling). This results in the sequence of lakes having a fractal structure, but at a relatively low "degree", which cannot be seen in Fig. 11. We shall say that the lakes have a "*light*" *fractal structure.*

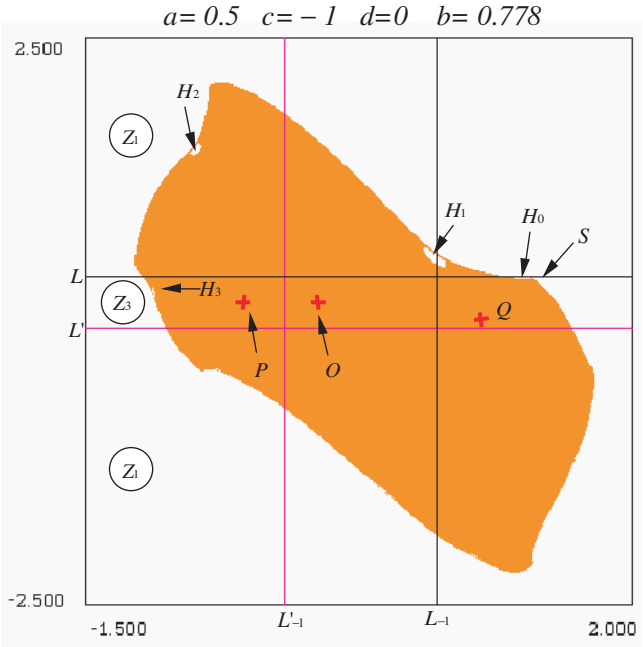

Fig. 11. Map T with $a = 0.5$, $b = 0.778$, $c = -1$, $d = 0$. The basin D is multiply connected. This results from a tangential contact of ∂D with the critical line L, at a local minimum of the ordinate of the external boundary ∂D, occurring for $b = b_{f4} \simeq 0.76574$. This bifurcation creates a bay H_0, a rank-one lake $H_1 = T^{-1}(H_0)$. The rank-$(n+1)$ lakes $T^{-n}(H_1) = H_{n+1}^{i_1 \cdots i_n}$, $n = 1, 2, \ldots$, form an incomplete arborescent sequences when $n \to \infty$. The limit set of the lakes $H_{n+1}^{i_1 \cdots i_n}$ is essentially made up of the external boundary $\partial_e D$, on which the cycles have a fractal structure.

The bifurcation $b = b_{f4}$ changes the simply connected basin D into a "light" fractal multiply connected one.

For $b = b_{f5} \simeq 0.789$ a contact between L and the external boundary $\partial_e D$ occurs in a small neighborhood of the unstable focus F^6. This contact bifurcation represents the destruction of the bay H_0, as for $b > b_{f5}$ the sea "penetrates" the lakes which become *roadsteads* [Mira *et al.*, 1996a] $R_{n+1}^{i_1 \cdots i_n}$, $n = 1, 2, \ldots$, (Fig. 12, $b = 0.8$).

The bifurcation occurring at $b = b_{f5}$ changes the multiply connected basin D into a simply connected one, the cycles of the external boundary $\partial_e D$ having a fractal structure.

For $b = b_{f6} \simeq 0.8065$ another bifurcation occurs due to a contact between L and the boundary $\partial_e D$,

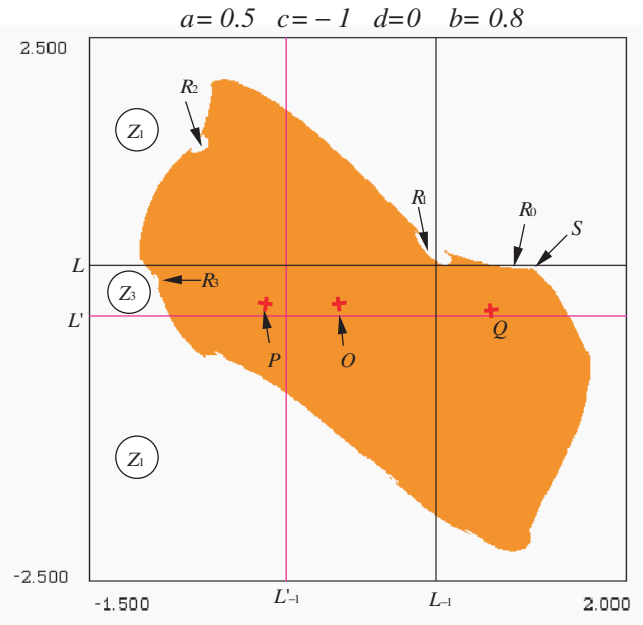

Fig. 12. Map T with $a = 0.5$, $b = 0.8$, $c = -1$, $d = 0$. For $b = b_{f5} \simeq 0.789$ a contact bifurcation between L and the external boundary $\partial_e D$ occurs at a local maximum S of the $\partial_e D$ ordinate. For $b = 0.8 > b_{f5}$ the bay H_0 no longer exists, and the lakes that become *roadsteads* R_n, $n = 1, 2, 3, \ldots$.

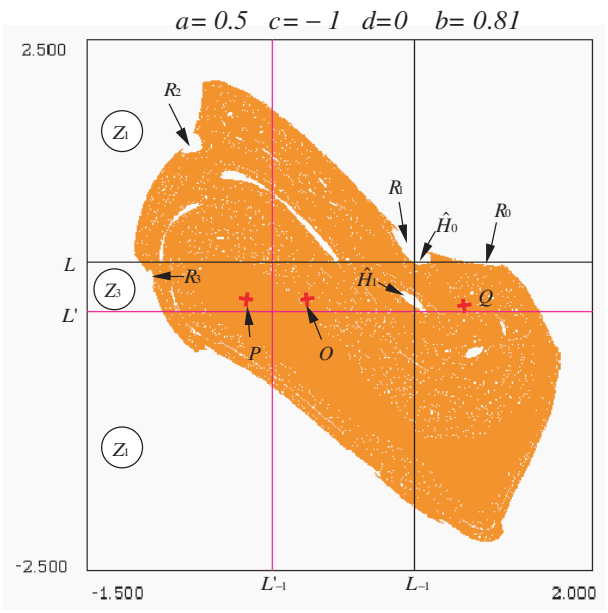

Fig. 13. Map T with $a = 0.5$, $b = 0.81$, $c = -1$, $d = 0$. For $b = b_{f6} \simeq 0.8065$ a contact bifurcation between L and the boundary $\partial_e D$ occurs at a local minimum of the $\partial_e D$ ordinate, inside the rank-one roadstead R_1. So a bay $\hat{H}_0 \subset R_1$ is created for $b > b_{f6}$, giving rise now to an arborescent sequence of lakes $T^{-n}(\hat{H}_1) = \hat{H}_{n+1}^{i_1 \cdots i_n}$, $n = 0, 1, 2 \ldots$. The limit set of the lakes $\hat{H}_{n+1}^{i_1 \cdots i_n}$, when $n \to \infty$, is made up of the strange repeller SR_1, and $\partial_e D$. So a hard change of the basin fractalization has occurred. The lakes have a "strong" fractal structure.

inside the rank-one roadstead R_1 (coming from the opening of the lake H_1). So a bay $\hat{H}_0 \subset R_1$ is created for $b > b_{f6}$, giving rise now to an arborescent sequence of lakes $T^{-n}(\hat{H}_1) = \hat{H}_{n+1}^{i_1 \cdots i_n}$, $n = 0, 1, 2, \ldots$. The lake $\hat{H}_1$, union of two rank-1 preimages of $\hat{H}_0$, belongs to Z_3 (see Fig. 13, obtained for $b = 0.81$), whereas the third inverse of $\hat{H}_0$ is an arc belonging to $\partial_e D$. The limit set of the lakes $\hat{H}_{n+1}^{i_1 \cdots i_n}$, when $n \to \infty$, is made up of the union of the strange repeller SR_1, and $SR_e \in \partial_e D$. So a hard change of the basin fractalization occurs. We shall say that the lakes have a "*strong*" *fractal structure.*

The bifurcation occurring at $b = b_{f6}$ *changes the simply connected basin* D, *with a "light" fractal external boundary* $\partial_e D$, *into a "strong" fractal multiply connected basin.*

When b increases from $b = b_{f6}$ the size of the lakes increases more and more inside the "continent" limited by $\partial_e D$, and more and more lakes of the same rank join after contact of some portions of the boundary of D with L or L'. Figure 14(a) (where $b = 0.82$) shows such a situation. With respect to Fig. 13, we can see that the (brown) area out of the (white) lakes reproduces the form of the former P basin, when the two attractors P and $\tilde{\Gamma}$ exist before the destabilization of the latter. Moreover

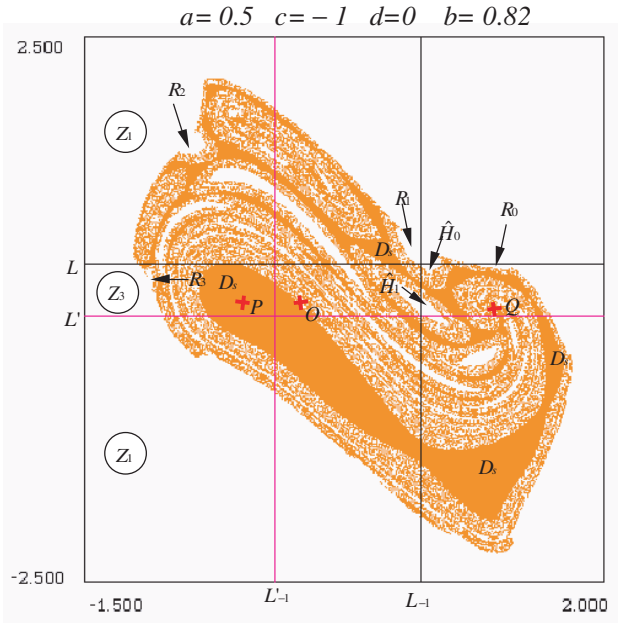

(a)

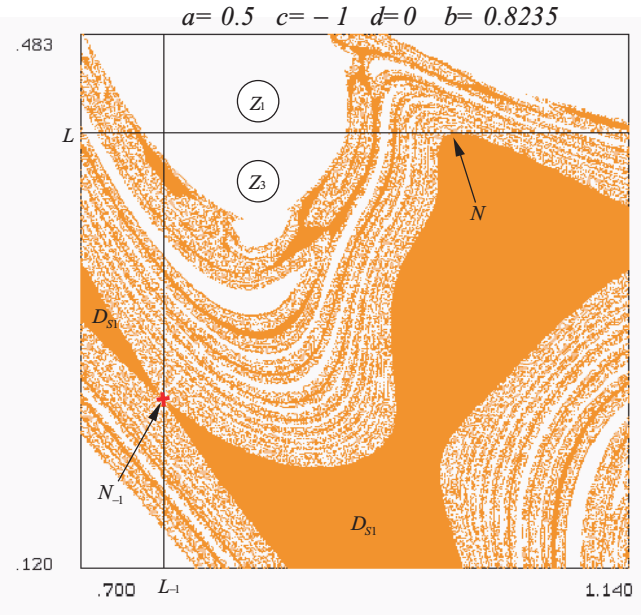

(b)

Fig. 14. (a) Map T with $a = 0.5$, $b = 0.82$, $c = -1$, $d = 0$. With respect to the Fig. 13 situation, the area out of the lakes set reproduces the form of the former P basin, when the two attractors P and $\tilde{\Gamma}$ existed. (b) $a = 0.5$, $b = 0.8235$, $c = -1$, $d = 0$. Enlargement showing the bifurcation leading to a contact of the basin boundaries ∂D_S and ∂D_{S1} at a point $N_{-1} \in L_{-1}$ when ∂D_S is tangent to L at the point N. This bifurcation separates the Figs. 14(a) and 15 situations.

the boundary of the brown region appears as limit set of increasing rank lakes with a laminated structure, the whole external boundary $\partial_e D$ being also a limit set of increasing rank lakes, but "spiraling" toward $\partial_e D$. This situation can be described as a "continent" a large part of which is occupied by an area with of higher and higher density of lakes when b increases. Such a typical situation will be called "*marshes*" *area* (the lakes set). For a better understanding we shall use the vague vocabulary "*firm soil*" for the brown region when it is not too narrow giving rise to a "laminated" structure. So the "firm soil" is first a connected domain $D_S \equiv D$ (Fig. 13).

When b increases D_S splits into nonconnected parts D_S (containing the point P), D_{Sn} (islands), $n = 1, 2, \ldots$, inside the "marshes" area, after contact between its boundary ∂D_S and L or L'. An example is given by the bifurcation situation represented by the enlargement of Fig. 14(b) ($b \simeq 0.8235$) leading to a contact of the basin boundaries ∂D_S and ∂D_{S1} at a point $N_{-1} \in L_{-1}$ when ∂D_S is tangent to L at the point N. This bifurcation separates the situations shown in Figs. 14(a) and 15. Note that in Fig. 15, D_{S1} is the result of the aggregation of nonconnected areas denoted $D_4^{3,i}$, $D_5^{3,i}$, D_3^{1-2}, D_6^{1-2} in Figs. 1(b) and 1(c) as D_S is the result of aggregation of nonconnected areas denoted D_0, D_1, D_n^3, $n = 2, 3, 4, \ldots$. At the bifurcation situation shown in Fig. 14(b), the contact of ∂D_S and ∂D_{S1} at N_{-1} occurs at the boundaries of $D_4^{3,1}$ (see also the qualitative picture in Fig. 1(b)), considered as aggregated to D_{S1}, and of D_5^3, considered as aggregated to D_S. The last splitting of D_S occurs for $b = b_{f7} \simeq 0.853$, with a contact between ∂D_S and L at the point M of Fig. 16 ($b = 0.853$), the qualitative representation being given in Fig. 1(c). For $b = b_{f7} - \varepsilon$, $\varepsilon > 0$ sufficiently small (Fig. 15), the qualitative conditions of Fig. 1(d) exist, the case of Fig. 1(b) corresponding to $b = b_{f7} + \varepsilon$, $\varepsilon > 0$ (Fig. 17, with $b = 0.86$). The enlargement of Fig. 18, shows islands as I made up of "marshes" surrounding a large part of "firm soil".

Remark. The transition from the situation shown in Fig. 13 to that shown in Fig. 17 has been described, for practical reasons, by using the image of a "marshes area" creation. In fact, infinitely many bifurcations by contact of one of the lakes boundary with L, or L', and also formation of small new bays, or headlands, occur without the possibility to have a precise view of the organization

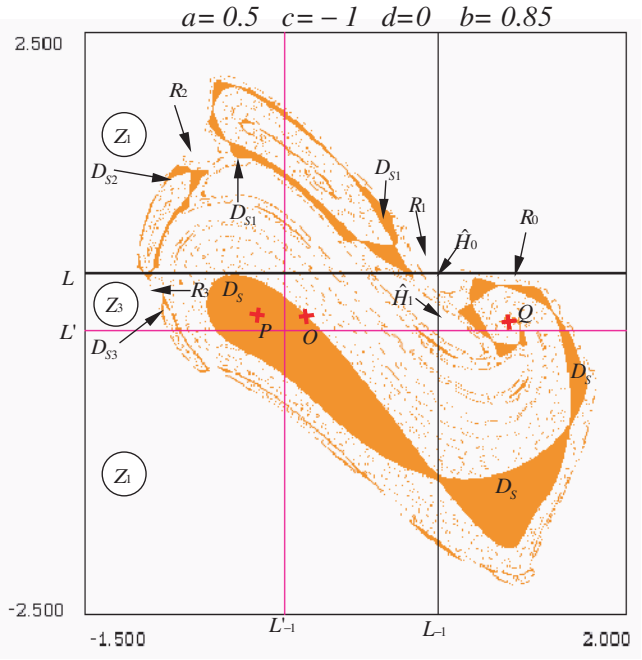

Fig. 15. Map T with $a = 0.5$, $b = 0.85$, $c = -1$, $d = 0$. From $b = 0.82$ progressively the immediate basin D_S splits into more and more islands, after contact between its boundary ∂D_S and L or L' according to the representation of Fig. 1(d).

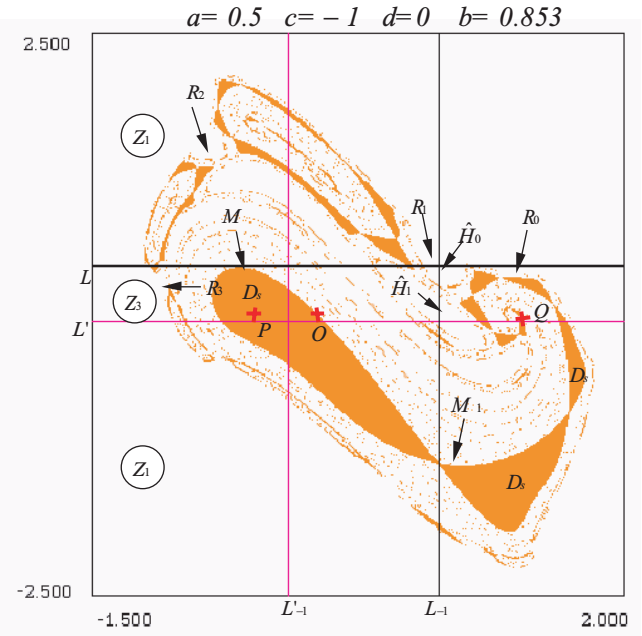

Fig. 16. Map T with $a = 0.5$, $b = b_{f7} \simeq 0.853$, $c = -1$, $d = 0$. The last splitting of D_S occurs for $b = b_{f7}$ with a contact between ∂D_S and L at the point M, the qualitative representation being given by Fig. 1(c).

of these bifurcations. A possible conjecture would be that one of these bifurcations would give a direct transition *multiply connected basin* $\rightarrow$ *nonconnected basin* in the presence of strange repellers SR_1 and

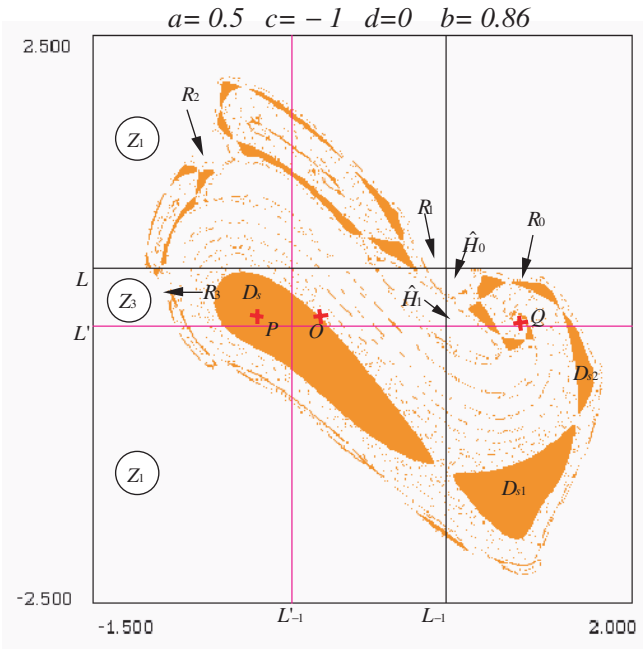

Fig. 17. Map T with $a = 0.5$, $b = 0.86$, $c = -1$, $d = 0$.

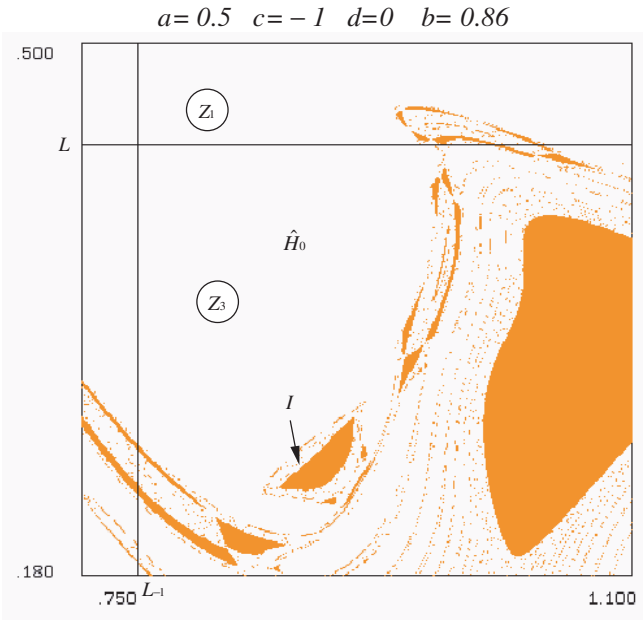

Fig. 18. Map T with $a = 0.5$, $b = 0.86$, $c = -1$, $d = 0$. Enlargement of Fig. 18.

SR_e as limit set, so differently from the description given in Sec. 4.2.

5.2. *Bifurcations in the presence of strange repellers. Second situation*

5.2.1. *Origin of the strange repellers*

We consider now the set of parameters $a = 0.25$, $c = -0.5$, $d = -1.08$, and b increasing in the range $1.08 \le b \le 1.25$. The fixed point O is an unstable node. The fixed point P is a stable node, and Q an unstable focus. The boundary ∂D of the domain D of bounded orbits contains cycles of period $4k \cdot 2^i$, $i = 0, 1, 2, \ldots$, $k = 1, 3, \ldots$, ($k = 1$ for b sufficiently close to 1.08). In particular, we consider the case of cycles of period $4k \cdot 2^i$ with $k = 3$. Let us consider, again, the one-dimensional map T_r, restriction of T to the repelling invariant closed curve ∂D. On this closed curve the dynamics is chaotic, and the set of cycles of period $4k \cdot 2^i$, as well as their increasing rank preimages, have a fractal structure. For $b = 1.08$ (Fig. 19), the map T has three attractors: the stable node P, a chaotic area (d), and a two-cyclic chaotic attractor $(\overline{d}) = (\overline{d}'_1) \cup (\overline{d}'_2)$. Their basins are respectively $D(P)$ (red) $D(d)$ (green) and $D(\overline{d})$ (yellow). The basin D is the union of these three basins, i.e. $D = D(P) \cup D(d) \cup D(\overline{d})$. The common boundary $\partial D(P) \cap \partial D(\overline{d})$ is made up of the stable manifold $W^s(C_2^j)$, $j = 1, 2$, of a period two saddle C_2^1, C_2^2. The two attractors (d) and $(\overline{d})$ are bounded by arcs of critical curves up to a certain

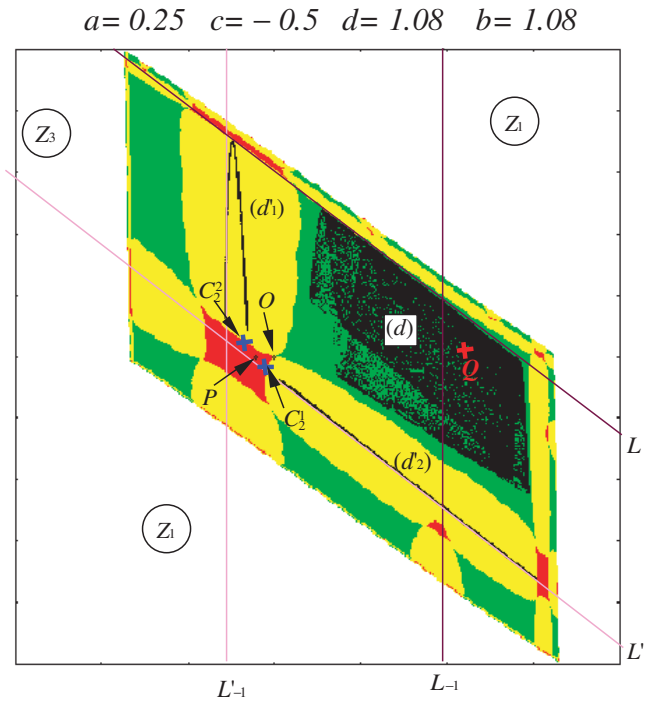

Fig. 19. Map T with $a = 0.25$, $b = 1.08$, $c = -0.5$, $d = -1.08$. The fixed point O is an unstable node. The fixed point P is a stable node, and Q an unstable focus. The map T has three attractors: the stable node P, a chaotic area (d), and a period two chaotic attractor $(\overline{d}) = (\overline{d}'_1) \cup (\overline{d}'_2)$. Their basins are respectively $D(P)$ (red colored) $D(d)$ (green) and $D(\overline{d})$ (yellow). The basin D is the union of these three basins $D = D(P) \cup D(d) \cup D(\overline{d})$.

rank [Mira *et al.*, 1996a]. A large segment of the critical curve L belongs to the boundary of (d). The common boundaries $\partial D(d) \cap \partial D(\overline{d})$ are made up of arcs, two of which have O as extremity and contain period $2k \cdot 2^i$ cycles, $i = 1, 2, \ldots$, $k = 1, 3, \ldots$. The dynamics are chaotic on these two arcs. The external boundary of the basins $D(P)$, $D(d)$, and $D(\overline{d})$ (limit set of the n-rank preimages of their immediate basins, when $n \to \infty$) is $\partial_e D$, when the dynamics are chaotic as well. The structure of these basins is simple, even if the restriction of the map to their boundaries may have complex dynamics.

For $b = b_{f8} \simeq 1.09172$ a contact bifurcation between the chaotic attractor $(\overline{d})$ and the stable manifold $W^s(C_2^j)$ occurs. This is a homoclinic bifurcation, due to a tangency of $W^s(C_2^j)$ with the branch of the unstable manifold $W^u(C_2^j)$ tending toward $(\overline{d})$. Then $(\overline{d})$ is destroyed for $b = b_{f8} + \varepsilon$, $\varepsilon > 0$ small, and gives rise to a strange repeller SR_1. Figure 20 ($b = 1.092$) shows the basins $D(P)$ and $D(d)$. The "granular" region (obtained with a small number of iterations for each pixel) inside $D(P)$ reproduces the former basin $D(\overline{d})$. It is an area of chaotic transient toward P, due to the presence of the chaotic repeller SR_1. It can be noticed that the chaotic area (d) is very close to its basin boundary $\partial D(d)$, so we are close to a contact bifurcation which will destroy (d). This bifurcation, also an homoclinic one, occurs for $b = b_{f9} \simeq 1.0935$. Figure 21 ($b = 1.0945$) shows the basin of the only attractor (the fixed point P) which survives after the bifurcation. The "granular" region inside $D(P) = D$ (which is simply connected) reproduces the shape of the former basin $D(d)$. It is an area of chaotic transient toward P, due to the presence of a new strange repeller SR_2, that constitutes the skeleton of the just disappeared attractor (d). The boundary ∂D of the basin D of P, $\partial D = \partial_e D \cup SR_1 \cup SR_2$, is strongly fractal, but the basin is not fractal.

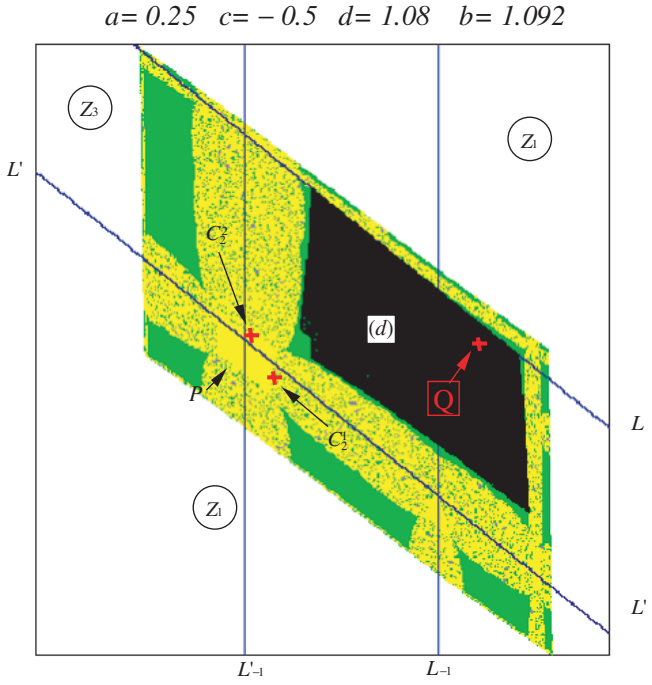

Fig. 20. Map T with $a = 0.25$, $b = 1.092$, $c = -0.5$, $d = -1.08$. Basins $D(P)$ and $D(d)$. For $b = b_{f8} \simeq 1.09172$ a contact bifurcation between the chaotic attractor $(\overline{d})$ and the stable manifold $W^s(C_2^j)$ has occurred. Then this bifurcation is destroyed $(\overline{d})$, giving rise to a strange repeller SR_1. The "granular" region inside $D(P)$ reproduces the ancient basin $D(\overline{d})$. It is an area of chaotic transient toward P, which corresponds to the presence SR_1. Note that the chaotic area (d) is very close to its basin boundary $\partial D(d)$, which means that we are near the contact bifurcation which will destroy (d).

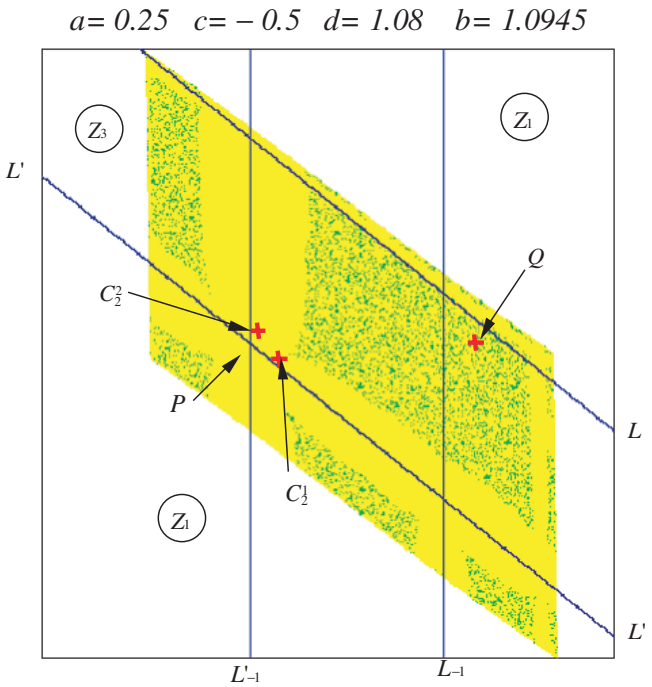

Fig. 21. Map T with $a = 0.25$, $b = 1.0945$, $c = -0.5$, $d = -1.08$. The bifurcation destroying (d), occurs for $b = b_{f9} \simeq 1.0935$. Only one attractor, the fixed point P, remains, the simply connected basin $D(P) = D$ of which is represented by the figure. The "granular" region reproduces the aspect of ancient basin $D(d)$. It is an area of chaotic transient toward P. This region corresponds to a new strange repeller SR_2, born from the destabilization of (d). The boundary ∂D of the basin D of P, $\partial D = \partial_e D \cup SR_1 \cup SR_2$, is strongly fractal, but the basin is not fractal.

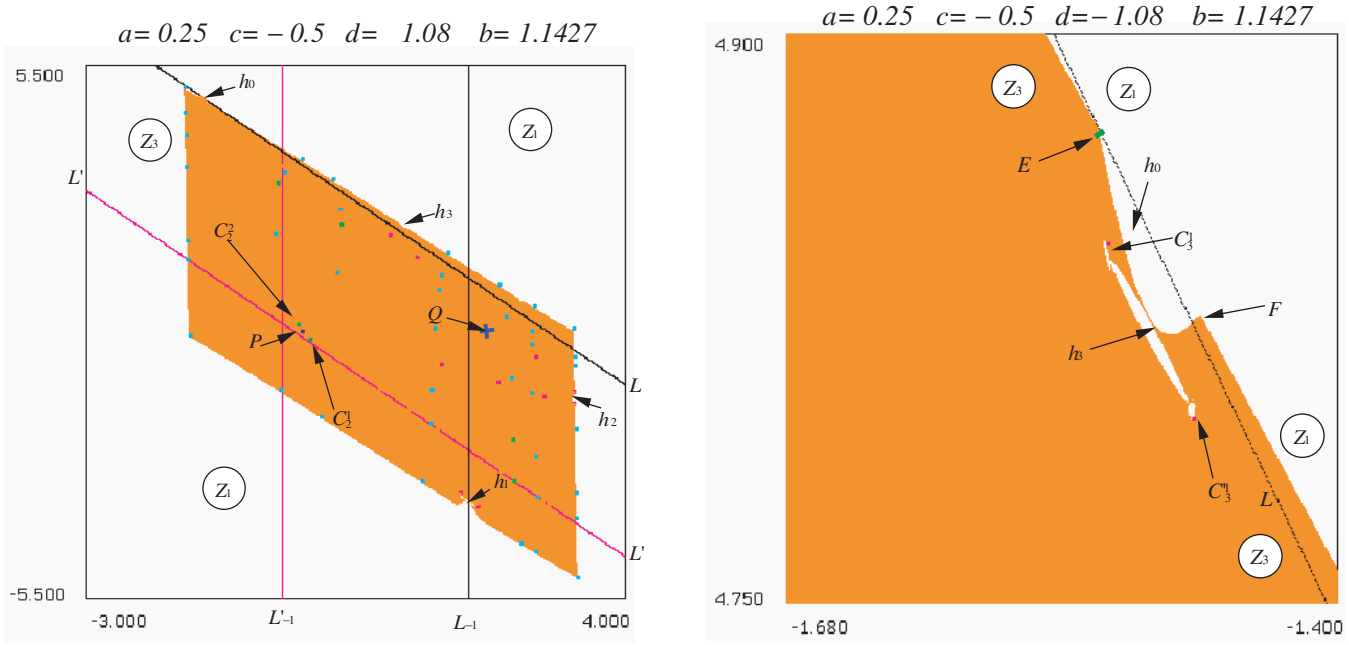

(a) (b)

(c)

Fig. 22. Map T with $a = 0.25$, $b = 1.1427$, $c = -0.5$, $d = -1.08$. (a) The basin D is now multiply connected. A bay h_0 has been generated via a tangential contact of $\partial_e D$ with the critical line L, at a local minimum of the $\partial_e D$ ordinate, when $b = b_{f10} \simeq 1.138$. The bay h_0 belongs to Z_3, and the rank-$n+1$ lakes $T^{-n}(h_1) = h_{n+1}^{i_1 \cdots i_n}$, $n = 1, 2, \ldots$, form an incomplete arborescent sequences when $n \to \infty$. (b) and (c) Enlargements showing the presence of two period three cycles C_3^j, $C_3'^j$, $j = 1, 2, 3$, belonging to the lakes limit set.

The bifurcations occurring at $b = b_{f8}$ and $b = b_{f9}$ respectively destroy the chaotic attractors $(\overline{d})$ and (d) with their basins. The final result is a simply connected nonfractal basin of the unique attractor P, the boundary of which ∂D is strongly fractal due to the presence of the two strange repellers SR_1 and SR_2 belonging to ∂D.

5.2.2. *Basin fractalization*

For $b = 1.1427$, a bay h_0 has been generated via a tangential contact of $\partial_e D$ with the critical line L when $b = b_{f10} \simeq 1.138$. So the basin D is now multiply connected (see Fig. 22(a), and the enlargements in Figs. 22(b) and 22(c)). The rank-one lake is $h_1 = T^{-1}(h_0)$, made up of the union of two preimages related to two different inverses of T. The third preimage of ∂h_0 gives an arc of $\partial_e D$. The bay h_0 belongs to Z_3, and the rank-$(n+1)$ lakes, $T^{-n}(h_1) = h_{n+1}^{i_1 \cdots i_n}$, $n = 1, 2, \ldots$, form an infinite sequence when $n \to \infty$. These lakes have essentially $\partial_e D$ as limit set, plus period $3k2^i$ unstable cycles, $i = 0, 1, 2, \ldots$, $k = 1, 3, \ldots$, inside the domain bounded by $\partial_e D$. The point E of Fig. 22(b) belongs to Z_1. Figures 22(a)–22(c) show the presence of two period three cycles C_3^j, $C_3'^j$, $j = 1, 2, 3$, belonging to the limit set. This results in the sequence of lakes having a fractal structure, because a fractal structure of repelling cycles exists on the boundary, that form the limit set of lakes, but at a relatively low "degree", which cannot be seen in Fig. 22. The lakes have a "*light*" *fractal structure.*

The bifurcation occurring at $b = b_{f10}$ changes the simply connected nonfractal basin D into a "light" fractal multiply connected one.

For $b = b_{f11} \simeq 1.1429$, the point E of $\partial_e D$ belongs to L. A contact bifurcation between L and the boundary $\partial_e D$ occurs. This contact bifurcation marks the destruction of the bay h_0. When $b > b_{f11}$ the sea "penetrates" the lakes, which become *roadsteads* [Mira *et al.*, 1996a] $B_{n+1}^{i_1 \cdots i_n}$, $n = 0, 2, \ldots$. When the point F of Fig. 22(b), belongs to Z_3, the roadsteads have "crossed" through the "former lakes", and we have the situation shown in Fig. 23, obtained for $b = 1.16$.

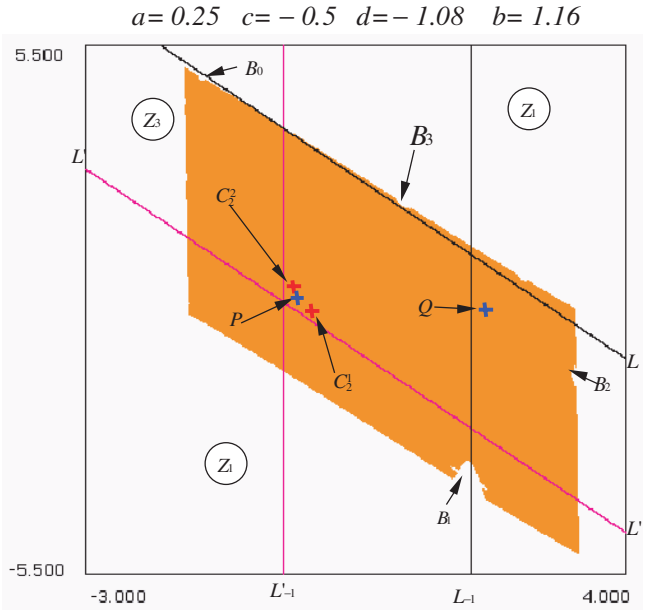

Fig. 23. Map T with $a = 0.25$, $b = 1.16$, $c = -0.5$, $d = -1.08$. For $b = b_{f11} \simeq 1.1429$, a contact bifurcation between L and the boundary $\partial_e D$ has occurred, the point E of $\partial_e D$ belonging to L (existence limit for the bay h_0). For $b = 1.16 > b_{f11}$ the lakes, which become *roadsteads* $B_{n+1}^{i_1 \cdots i_n}$, $n = 0, 2, \ldots$. Moreover for $b = 1.16$ the point F of Fig. 22(b) belongs to Z_3, and the roadsteads have "crossed" through the "ancient" lakes.

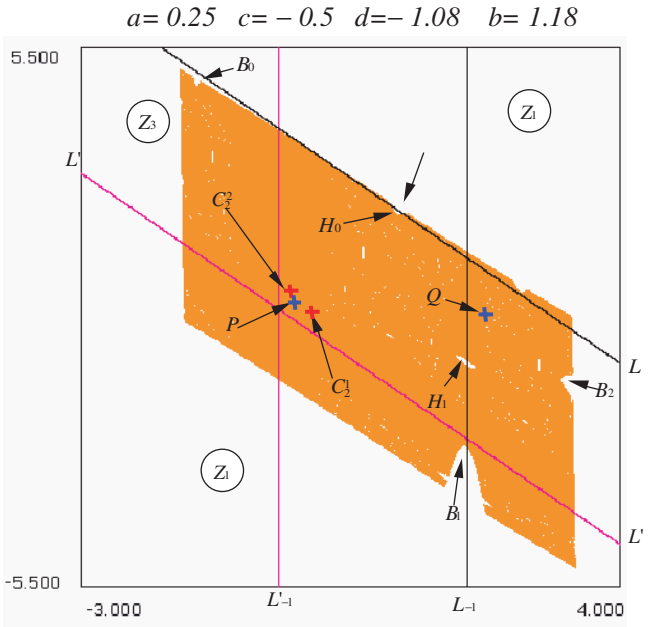

Fig. 24. Map T with $a = 0.25$, $b = 1.18$, $c = -0.5$, $d = -1.08$. A contact of a local minimum of roadstead boundary ∂B_3 with L, has occurred for $b = b_{f12} \simeq 1.1754$. So for $b = 1.18 > b_{f12}$ the simply connected basin D turns into a multiply connected one. A bay $H_0 \subset B_3$ has been generated. The rank-one lake is $H_1 = T^{-1}(H_0)$, made up of the union of two inverses of T. It belongs to Z_3, and the rank-$n+1$ lakes $T^{-n}(H_1) = H_{n+1}^{i_1 \cdots i_n}$, $n = 1, 2, \ldots$, form now a complete arborescent sequence when $n \to \infty$. These lakes have $SR_2 \cup \partial_e D$ as limit set. They "reproduce" the form of the ancient basin $D(d)$, now they have a "*strong*" *fractal structure.*

The bifurcation occurring at $b = b_{f11}$ *changes the multiply connected "light" fractal basin* D *into a simply connected one, the external boundary* $\partial_e D$ *being "light" fractal.*

It can be noticed that the roadstead $B_3 \subset T^{-3}(B_0)$ is near the critical line L, a situation leading to the creation of a bay. This occurs after a contact of ∂B_3 with L, occurring for $b = b_{f12} \simeq 1.1754$. The simply connected basin D turns into a multiply connected one. Figure 24 shows the dynamic situation obtained for $b = 1.18$. A bay $H_0 \subset B_3$ has been generated. The rank-one lake is $H_1 = T^{-1}(H_0)$, made up of the union of two preimages of H_0. The third preimage of ∂H_0 gives an arc of $\partial_e D$. The lake H_1 belongs to Z_3, and the rank-$n+1$ lakes $T^{-n}(H_1) = H_{n+1}^{i_1 \cdots i_n}$, $n = 1, 2, \ldots$, form an infinite sequence when $n \to \infty$, with many preimages in Z_3. As Fig. 24 shows, these lakes have $SR_2 \cup \partial_e D$ as limit set, i.e. the external boundary $\partial_e D$ of D, and the strange repeller born from the destabilization of the chaotic area (d). They "reproduce" the form of the ancient basin $D(d)$. These lakes now have a "*strong*" *fractal structure.* The boundary $\partial_e D$ undergoes a qualitative change because now cycles of period different from $4k2^i$ cycles, $i = 0, 1, 2, \ldots$, $k = 1, 3, \ldots$, belong to this boundary, in particular, it contains a pair of period three, six and nine cycles coming from the limit set of the lakes h_n after their opening in the sea. These cycles are located on arcs of roadstead B_n, $n = 1, 2, 3$.

The bifurcation occurring at $b = b_{f12}$ *changes the simply connected basin* D*, with a "light" fractal external boundary* $\partial_e D$*, into a "strong" fractal multiply connected basin.*

Again, the fact that the roadstead B_1 is close to the critical line L' announces the possible creation of a new bay. This occurs for $b = b_{f13} \simeq 1.18385$. Figures 25(a) and 25(b) show the new situation obtained for $b = 1.19$. A bay $\hat{H}_0 \subset B_1$ has been generated and a new sequence of lakes exists, many of which belong to Z_3. The first one $\hat{H}_1 = T^{-1}(\hat{H}_0)$ is made up of the union of two preimages of $\hat{H}_0$. The third preimage of $\partial \hat{H}_0$ gives an arc of $\partial_e D$. The lake $\hat{H}_1$ belongs to Z_3. As shown in Fig. 25(a), these new lakes have $SR_1 \cup \partial_e D$ as limit set, i.e.

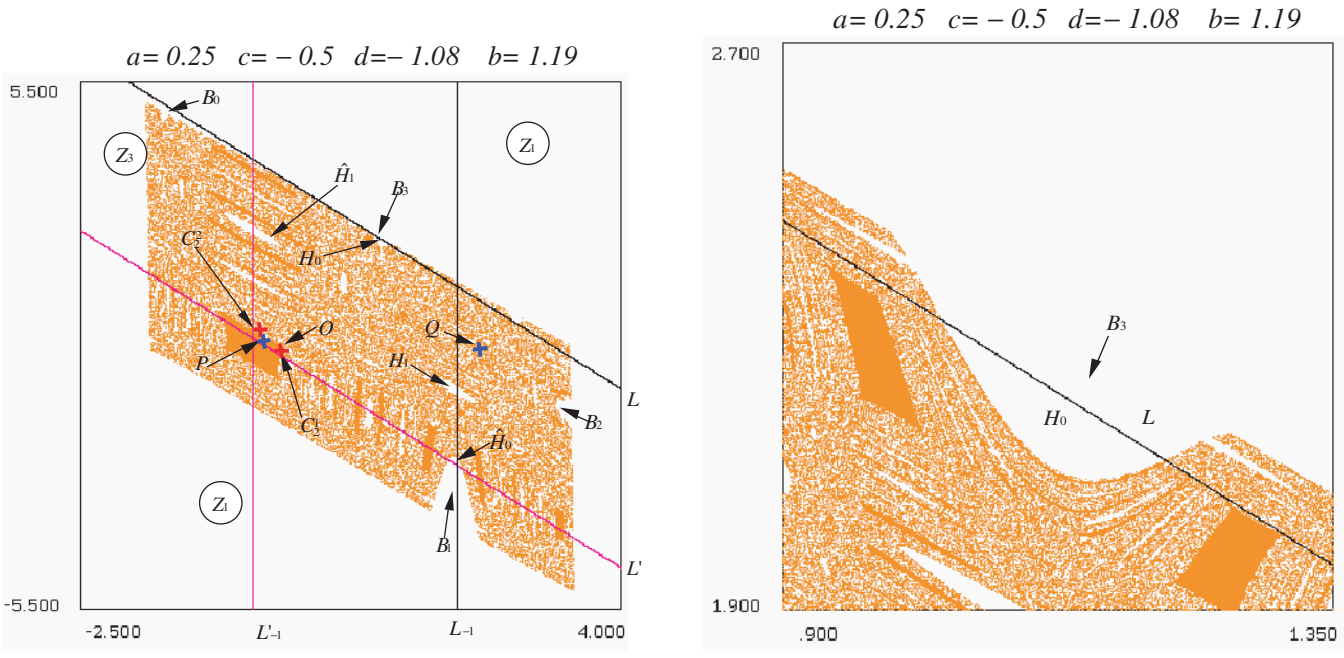

(a) (b)

Fig. 25. Map T with $a = 0.25$, $b = 1.19$, $c = -0.5$, $d = -1.08$. (a) A new bay $\hat{H}_0 \subset B_1$ has been created from the bifurcation $b = b_{f13} \simeq 1.18385$, corresponding to the contact between the critical line L' and the roadstead boundary ∂B_1 at a local maximum of ∂B_1. A new complete arborescent sequence of lakes exists, the first one being $\hat{H}_1 = T^{-1}(\hat{H}_0)$ made up of the union of two inverses of T, and belonging to Z_3. These new lakes have $SR_1 \cup \partial_e D$ as limit set, i.e. the strange repeller born from the destabilization of the chaotic area $(\overline{d})$ and the external boundary of D. They "reproduce" the form of the ancient basin $D(\overline{d})$. The association of the two lakes sequences, with the limit set $SR_1 \cup SR_2 \cup \partial_e D$, gives rise to a new "*strong*" *fractal structure* of the D basin with a higher degree of "strength". (b) Enlargement of a part of Fig. 25(a).

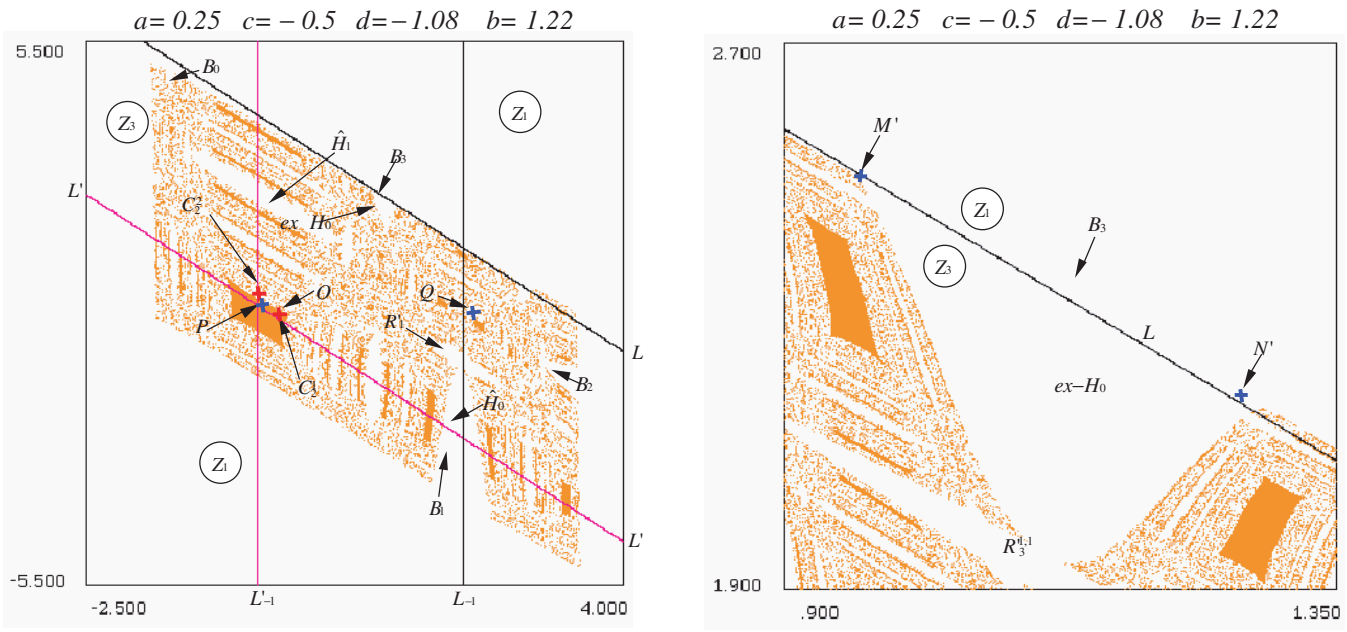

(a) (b)

Fig. 26. Map T with $a = 0.25$, $b = 1.19$, $c = -0.5$, $d = -1.08$. (a) For $b = b_{f14} \simeq 1.219$ a contact bifurcation between L and the boundary $\partial_e D$ has occurred at the point $M' \in L$, with $N' \in Z_1$. For $b = 1.19 > b_{f14}$, the lake H_1 communicates with B_1, forming a new roadstead R'_1. Then all the lakes of the arborescent sequence, having $SR_2 \cup \partial_e D$ as limit set, communicate with the sea. (b) Enlargement of a part of Fig. 26(a). H_0 is no longer a bay (exH_0 in the figure), and the lake $H_3^{1,1}$ has turned in a roadstead $R_3'^{1,1}$.

the strange repeller born from the destabilization of the chaotic area ($\overline{d}$) and the external boundary of D. They "reproduce" the form of the former basin $D(\overline{d})$. The association of the two lake sequences, with the limit set $SR_1 \cup SR_2 \cup \partial_e D$, gives rise to a new "*strong*" *fractal structure* of the D basin with a higher degree of "strength". As in Sec. 5.1.2, this situation can be described as a "continent" a large part of which is occupied by a "*marshes*" *area* (the lakes set).

The bifurcation occurring at $b = b_{f13}$ *changes the "strong" fractal multiply connected basin* D *into a "stronger" fractal multiply connected one.*

For $b = b_{f14} \simeq 1.219$ a contact bifurcation between L and the boundary $\partial_e D$ occurs at a point M' one of the two "extremities" of the roadstead B_3, $M' \in L$, the other "extremity" $N' \in Z_1$. For $b = b_{f14} + \varepsilon$, $\varepsilon > 0$ small, the lake H_1 communicates with B_1, forming a new roadstead R'_1. Then all the lakes of the arborescent sequence, having $SR_2 \cup \partial_e D$ as limit set, communicate with the sea (see Figs. 26(a) and 26(b). In Fig. 26(b) we see that $M' \in Z_3$, $N' \in Z_1$. H_0 is no longer a bay, and the lake $H_3^{1,1}$ has turned in a roadstead $R_3'^{1,1}$.

Crossing through the bifurcation value $b = b_{f14}$, *the "strong" fractal multiply connected basin* D *loses all the lakes having the strange repeller* SR_2 *as limit set. Now* SR_2 *belongs to the external boundary* $\partial_e D$. *So* $\partial_e D$ *now has a "higher degree" of fractalization with respect to the one existing before the bifurcation.*

The same remark as that at the end of Sec. 5.1.2 can be made. The transition from the situation shown in Fig. 24 to the one shown in Fig. 25 can be explained by the conjecture of a bifurcation that gives a direct transition *multiply connected basin* → *nonconnected basin* in the presence of strange repellers SR, SR_2, SR_e as limit sets.

6. Conclusion

This paper has shown that, depending on the position of a basin boundary with respect to the critical set LC, a lot of different situations are possible, the contact of these two sets giving rise to several kinds of bifurcations. The remarkable diversity of

these situations is related to a very large variety of structures of basin boundaries when they are fractal. The publications quoted in the references have already evidenced these circumstances in relatively simple cases. With respect to them, this paper shows that such contact bifurcations can change the nature of a fractal basin, i.e. its "degree" of fractalization. Such a degree results from the properties of a *strange repeller*, limit set of elements of nonconnected basins, or multiply connected ones. When a strange repeller appears, in particular as a limit set of a nonconnected basin, or a multiply connected one, we are in the situation described in Sec. 2.4, and homoclinic tangencies are dense by varying a parameter after a first homoclinic tangency. This means that the parameter space of (1) contains *Newhouse regions*. Indeed the strange repellers generated by (1) contains saddle cycles, the basin boundaries include stable manifold of saddle cycles. At the actual stage, we are far from a complete study of all the dynamic situations and bifurcations.

The results of this paper allow us to get an insight into some properties of the family of three-dimensional diffeomorphisms obtained by imbedding the two-dimensional noninvertible map (1) into this diffeomorphism, for example in the form:

$$\begin{aligned} x' &= x + y \\ y' &= ax + bx^2 + cx^3 + dy + z \\ z' &= \mu(x + y) \end{aligned}$$

according to the process described in [Mira & Gracio, 2004].

References

Bischi, G. I., Gardini, L. & Mira, C. [1999] "Maps with denominator. Part 1: Some generic properties," *Int. J. Bifurcation and Chaos* **9**, 119–153.

Cathala, J. C. [2003] "About a class of invariant areas generated by two-dimensional endomorphisms," *Int. J. Bifurcation and Chaos* **13**, 905–933.

Frouzakis, C. E., Gardini, L., Kevrekidis, I. G., Millerioux, G. & Mira, C. [1997] "On some properties of invariant sets of two-dimensional noninvertible maps," *Int. J. Bifurcation and Chaos* **7**, 1167–1194.

Gumowski, I. & Mira, C. [1980a] *Dynamique Chaotique* (Cépadues Editions Toulouse, 1980).

Gumowski, I. & Mira, C. [1980b] *Recurrences and Discrete Dynamic Systems*, Lecture Notes in Mathematics, Vol. 809 (Springer-Verlag).

Millérioux, G. & Mira, C. [1997] "Homoclinic and heteroclinic situations specific to two-dimensional noninvertible maps," *Int. J. Bifurcation and Chaos* **7**, 39–70.

Mira, C. [1987] *Chaotic Dynamics. From the One-Dimensional Endomorphism to the Two-Dimensional Diffeomorphism* (World Scientific, Singapore), 450 pp.

Mira, C., Fournier-Prunaret, D., Gardini, L., Kawakami, H. & Cathala, J. C. [1994] "Basin bifurcations of two-dimensional noninvertible maps: Fractalization of basins," *Int. J. Bifurcation and Chaos* **4**, 343–381.

Mira, C., Gardini, L., Barugola, A. & Cathala, J. C. [1996a] *Chaotic Dynamics in Two-Dimensional Noninvertible Maps*, World Scientific Series on Nonlinear Sciences, Series A, Vol. 20, 630 pp.

Mira, C., Millerioux, G., Carcasses, J. P. & Gardini, L. [1996b] "Plane foliation of two-dimensional noninvertible maps," *Int. J. Bifurcation and Chaos* **6**, 1439–1462.

Mira, C. & Gracio, C. [2004] "On the embedding of a $(p-1)$-dimensional noninvertible map into a p-dimensional invertible map $(p = 2, 3)$," *Int. J. Bifurcation and Chaos* **13**, 1787–1810.

Sharkovskij, A. N. [1969] "Problem of isomorphism of dynamical systems," *Proc. 5th. Int. Conf. Nonlinear Oscillations, Kiev*, Vol. 2, pp. 541–544.

Shilnikov, L. P. [1997] "Mathematical problem of nonlinear dynamics: A tutorial," *Int. J. Bifurcation and Chaos* **7**, 1953–2001.